

# research report

## **Analytical Equations for Critical Local Buckling Stress of Lipped Channels**

**RESEARCH REPORT RP23-01**

**May 2023**



**American Iron and Steel Institute**

**DISCLAIMER**

The material contained herein has been developed by researchers based on their research findings and is for general information only. The information in it should not be used without first securing competent advice with respect to its suitability for any given application. The publication of the information is not intended as a representation or warranty on the part of the American Iron and Steel Institute or of any other person named herein, that the information is suitable for any general or particular use or of freedom from infringement of any patent or patents. Anyone making use of the information assumes all liability arising from such use.



# **Analytical Equations for Critical Local Buckling Stress of Lipped Channels**

April 2023

Chu Ding, PhD

Benjamin W. Schafer, PhD

Johns Hopkins University

COLD-FORMED STEEL RESEARCH CONSORTIUM  
REPORT SERIES  
**CFSRC R-2023-02**

## **Acknowledgements**

This research is supported by the American Iron and Steel Institute (AISI) and the Steel Framing Industry Association (SFIA) small project/fellowship program. Any opinions, findings, and conclusions or recommendations expressed in this publication are those of the author(s) and do not necessarily reflect the views of the American Iron and Steel Institute and Steel Framing Industry Association. The authors would like to thank Muhie Dean Ahdab and Astrid Fischer for the preliminary study related to this project and Bob Glauz for advice on the specification ballot process.

## **CFSRC information**

The Cold-Formed Steel Research Consortium (CFSRC) is a multi-institute consortium of university researchers dedicated to providing world-leading research that enables structural engineers and manufacturers to realize the full potential of structures utilizing cold-formed steel. More information can be found at [www.cfsrc.org](http://www.cfsrc.org). All CFSRC reports are hosted permanently by the Johns Hopkins University library in the DSpace collection:  
<https://jsscholarship.library.jhu.edu/handle/1774.2/40427>.

## **Abstract**

The objective of this study is to develop accurate analytical equations for calculating the critical local buckling stress of lipped channels with or without punchouts under compression and bending. Finite strip analysis is conducted on over 1000 lipped channel sections under four different loading conditions. Simple polynomial ratio equations are fit to the finite strip analysis results. The performance of the developed expressions are compared against the finite strip analyses and the element method currently provided in the AISI S100 Specification. The developed expressions are intended for use by engineers in future versions of the AISI S100 Specification.

## Table of Contents

Abstract.....	3
List of Tables .....	5
List of Figures.....	5
1   Introduction.....	7
2   Current analytical method in AISI S100 .....	8
3   Finite strip analysis for developing analytical equations.....	9
4   Critical buckling local stress from FSM .....	10
5   Plate buckling coefficients from FSM.....	11
6   Sections without punchouts .....	12
6.1   Pure compression.....	12
6.2   Major axis bending .....	14
6.3   Minor axis bending with lip in compression .....	16
6.4   Minor axis bending with lip in tension.....	20
7   Sections with standard web punchouts .....	22
7.1   Determine critical local buckling load/moment .....	22
8   Determine critical local buckling stress.....	23
8.1   Pure compression.....	24
8.2   Major axis bending .....	27
8.3   Minor axis bending with lip in compression .....	30
8.4   Minor axis bending with lip in tension.....	30
9   Summary of performance of proposed equations.....	33
10   Summary of proposed equations .....	34
11   Design examples.....	36
11.1   Sections without punchouts .....	36
11.1.1 Design example 1: 550S162-54 under pure compression .....	36
11.1.2 Design example 2: 800S250-43 under major axis bending .....	37
11.1.3 Design example 3: 362S137-33 under minor axis bending with lip in compression .....	37
11.2   Sections with standard punchouts.....	38
11.2.1 Design example 4: 550S162-54 with standard web punchout under pure compression .....	38
11.2.2 Design example 5: 800S250-43 with standard web punchout under major axis bending.....	39
12   Conclusions.....	40
Appendix A. Dimensions of non-commercial sections used in FSM analysis.....	40
References.....	61

## List of Tables

Table 1. Summary of the performance of the proposed equations for sections without holes .....	33
Table 2. Summary of the performance of the proposed equations for sections with standard web punchout .....	33
Table 3. List of proposed equations for lipped channels without punchouts .....	34
Table 4. List of proposed equations for lipped channels with standard web punchouts .....	35
Table 5. Dimensions of the non-commercial sections used in this study .....	40

## List of Figures

Fig. 1. Typical CFS lipped channel section, annotated with out-to-out dimensions $H$ , $B$ , and $D$ , inside corner radius $r$ , and uncoated thickness $t$ .....	7
Fig. 2. Finite strip model of lipped channel sections .....	10
Fig. 3. Centerline dimensions of lipped channel sections .....	10
Fig. 4. The proposed equation for gross lipped channel sections under pure compression against FSM results .....	13
Fig. 5. Histogram of the prediction accuracy of the proposed equation for gross lipped channel section under pure compression .....	13
Fig. 6. The proposed equation for gross lipped channel sections under major axis bending against FSM results .....	15
Fig. 7. Histogram of the prediction accuracy of the proposed equation for gross lipped channel section under major axis bending .....	15
Fig. 8. Dependency of the buckling coefficient of minor-axis bending with lip in compression on geometric ratio and stress gradient .....	16
Fig. 9. Comparisons between the relationship between buckling coefficient and stress gradient at different geometric ratios for lipped channel sections under minor axis bending with lip in compression .....	17
Fig. 10. Stress gradient multiplier against geometric ratio for lipped channel sections under minor axis bending with lip in compression .....	18
Fig. 11. The proposed equation for gross lipped channel sections under minor axis bending with lip in compression against FSM results .....	19
Fig. 12. Histogram of the prediction accuracy of the proposed equation for gross lipped channel section under minor axis bending with lip in compression .....	20
Fig. 13. The proposed equation for gross lipped channel sections under minor axis bending with lip in tension against FSM results .....	21
Fig. 14. Histogram of the prediction accuracy of the proposed equation for gross lipped channel section under minor axis bending with lip in tension .....	21
Fig. 15. Dimensions of standard web punchout .....	23
Fig. 16. Comparing the proposed equation for unrestrained buckling coefficients against FSM results for lipped channel sections with punchout under pure compression .....	25
Fig. 17. Comparing the proposed equation for the effect of punchout length restraint against FSM results for lipped channel sections with punchout under pure compression .....	25
Fig. 18. Histogram of the prediction accuracy of the proposed equation for lipped channel sections with punchouts under pure compression without considering punchout length .....	26
Fig. 19. Histogram of the prediction accuracy of the proposed equation for lipped channel sections with punchouts under pure compression .....	26
Fig. 20. Comparing the proposed equation for unrestrained buckling coefficients against FSM results for lipped channel section with punchout under major axis bending .....	28

Fig. 21. Comparing the proposed equation for the effect of punchout length restraint against FSM results for lipped channel section with punchout under major axis bending .....	28
Fig. 22. Histogram of the prediction accuracy of the proposed equation for lipped channel sections with punchouts under major axis bending without considering punchout length .....	29
Fig. 23. Histogram of the prediction accuracy of the proposed equation for lipped channel sections with punchouts under major axis bending .....	29
Fig. 24. Histogram of the prediction accuracy of the proposed equation for lipped channel sections with punchouts under minor axis bending with lip in compression .....	30
Fig. 25. Comparing the proposed equation for unrestrained buckling coefficients against FSM results for lipped channel section with punchout under minor axis bending with lip in tension.....	31
Fig. 26. Comparing the proposed equation for the effect of punchout length restraint against FSM results for lipped channel sections with punchout under minor axis bending in tension.....	32
Fig. 27. Histogram of the prediction accuracy of the proposed equation for lipped channel sections with punchouts under minor axis bending with lip in tension without considering punchout length .....	32
Fig. 28. Histogram of the prediction accuracy of the proposed equation for lipped channel sections with punchouts under minor axis bending with lip in tension .....	33

# 1 Introduction

A lipped channel is one of the most common sections in the cold-formed steel (CFS) framing industry. The strength of a CFS lipped channel is controlled by the minimum strength across several types of buckling, one of which is local buckling. The Direct Strength Method (DSM) in AISI S100 (2020) may be used for designing against local buckling, and requires the input of the cross-section critical local buckling stress by the engineer.

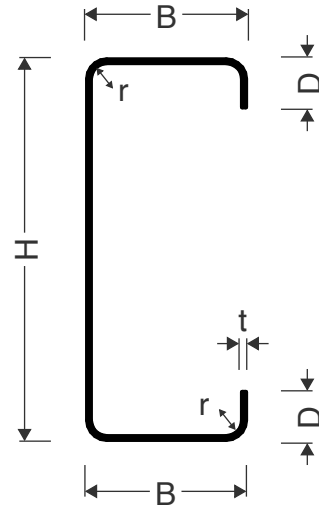


Fig. 1. Typical CFS lipped channel section, annotated with out-to-out dimensions  $H$ ,  $B$ , and  $D$ , inside corner radius  $r$ , and uncoated thickness  $t$ .

Engineers employing DSM in AISI S100 are referred to Appendix 2 for determining the elastic buckling stress. Appendix 2 makes it clear either of two methods, fully detailed, may be used by the engineer: (1) the element method which uses single plate element local buckling stresses, and (2) numerical methods by finite strip (discussed in the greatest detail) or shell finite element analysis. However, despite the merits, each method has its own limitations. The element method is convenient to use but can be overly conservative, because it does not properly consider interactions amongst the adjacent plates that comprise a cross-section. Additionally, the method is limited in the consideration of punchouts, e.g., not considering punchout length. On the other hand, numerical methods such as the finite strip analysis provide an accurate answer, but can be less convenient in practice, requiring a change in workflow and placing an analysis within the loop for calculating basic member strength. An alternative method, which is both accurate and convenient would be desirable.

The finite strip method has been used as a basis in the past for development of analytical equations for buckling stress. By fitting equations to finite strip analysis results, the equations developed can properly consider adjacent plate interactions. Seif and Schafer (2010) and Gardner et al. (2019) proposed analytical equations for critical local buckling stresses for a variety of hot-rolled structural steel shapes, which lead to improved accuracy over the equations used in AISC specifications and Eurocode. For cold-formed steel sections, de Miranda Batista (2010) proposed equations for buckling coefficients of several CFS sections under pure compression and major axis bending, and those equations were adopted in Brazilian CFS design code. More comprehensive coverage of loading conditions was conducted by Ahdab et al. (2022), which developed buckling coefficients equations for lipped channel sections under four types of loading (pure compression, major axis bending, minor axis bending with lip in tension, and minor axis

bending with lip in compression). However, so far, there has been only limited efforts on the development of analytical equations for CFS sections with web punchouts using finite strip analysis.

This study is aimed at developing a set of analytical equations for critical local buckling stresses of both gross (unpunched) lipped channel sections and ones with punchouts. The proposed analytical equations are expected to be both highly accurate and convenient to use.

## 2 Current analytical method in AISI S100

The current AISI S100 (2020) Appendix 2 provides analytical expressions of critical local buckling stresses  $F_{cr\ell}$  of individual plate elements of a cross section, e.g., web in a lipped channel section. Since  $F_{cr\ell}$  is calculated over individual elements instead of the whole section, this method is called the element method. The section-level  $F_{cr\ell}$  is the minimum  $F_{cr\ell}$  among all plate elements of a given cross-section.

There are two limitations with respect to the element method. First, it does not accurately consider the restraints (or demands) provided by adjacent plates. Second, the calculation can be overly involved. Calculation is required for each plate, and stresses from multiple plates need to be converted to the stresses at the same location to be compared.

The general equation for critical local buckling stress in AISI S100 (2020) is shown in Eq. (1).

$$F_{cr\ell} = k \frac{\pi^2 E}{12(1 - \mu^2)} \left(\frac{t}{w}\right)^2 \quad (1)$$

where  $k$  is the plate buckling coefficient,  $t$  is the plate thickness,  $w$  is the plate flat width,  $E$  is Young's modulus and  $\mu$  is Poisson's ratio. The effect of stress gradient and restraint by adjacent elements are considered through the plate buckling coefficient,  $k$ .

The expressions for the plate buckling coefficient are dependent on element stress distribution, plate boundary condition (stiffened vs. unstiffened) and plate type (flange vs. non-flange). The expressions for the buckling coefficients under various conditions utilized in AISI S100 are summarized herein.

For stiffened element under uniform compression from AISI S100 Section 1.1:

$$k = 4 \quad (2)$$

For unstiffened element under pure compression per AISI S100 Section 1.2.1:

$$k = 0.43 \quad (3)$$

For stiffened element under stress gradient  $\psi$ , per AISI S100 Section 1.1.2:

(1) For element with both compression and tension

$$k = 4 + 2(1 + \psi)^3 + 2(1 + \psi) \quad (4)$$

where  $\psi = |f_2/f_1|$ ,  $f_1$  is the compression stress and  $f_2$  is the tension stress

(2) For element with compression only

$$k = 4 + 2(1 - \psi)^3 + 2(1 - \psi) \quad (5)$$

where  $\psi = |f_2/f_1|$ ,  $f_2 \leq f_1$

For unstiffened element under stress gradient  $\psi$ , per AISI S100 Section 1.2.2:

(1) For element with compression only and stress decreases toward unsupported edge

$$k = 0.578/(\psi + 0.34) \quad (6)$$

where  $\psi = |f_2/f_1|$ ,  $f_2 \leq f_1$

(2) For element with compression only and stress decreases toward supported edge

$$k = 0.57 - 0.21\psi + 0.07\psi^2 \quad (7)$$

where  $\psi = |f_2/f_1|$ ,  $f_2 \leq f_1$

(3) For element with supported edge in tension and the unsupported edge is in compression

$$k = 0.57 + 0.21\psi + 0.07\psi^2 \quad (8)$$

where  $\psi = |f_2/f_1|$ ,  $f_1$  is the compression stress and  $f_2$  is the tension stress

(4) For element with supported edge in compression and the unsupported edge is in tension

$$k = 1.70 + 5\psi + 17.1\psi^2 \quad (9)$$

where  $\psi = |f_2/f_1|$ ,  $f_1$  is the compression stress and  $f_2$  is the tension stress

### 3 Finite strip analysis for developing analytical equations

Appendix 2 in AISI S100 (2020) provides another approach for determining cross-section critical local buckling stress: numerical analysis; specifically, finite strip analysis and shell finite element analysis. Among the two options, finite strip analysis is the least computationally expensive.

For the development of accurate analytical equations for critical local buckling stress, a numerical study using finite strip method (FSM) analysis is conducted. FSM analysis is performed on 1228 lipped channel cross-sections under four loading conditions. The 1228 lipped channels cross-sections include 244 SFIA (2018) commercial sections and 984 non-commercial sections. The non-commercial sections are created with the following geometric ratios: B/H between 0.05 and 0.75, D/B between 0.1 and 0.4, B/t > 8, and D/t > 4. The exact dimensions of the non-commercial sections are provided in Appendix A of this report. The four loading conditions include: pure compression, major-axis bending, minor-axis bending with lip in compression, and minor-axis bending with lip in tension.

The FSM analysis is conducted in CUFSM5, an open-source finite strip analysis software developed by Schafer (2020). For each lipped channel cross-section, two FSM models (Fig. 2) are created, one without punchout and one with standard web punchout. All FSM models are created using plate centerline dimension (Fig. 3). Round corners are modeled with at least 4 elements. For flat plates, a minimum of 8 elements are used for modeling the web plate, a minimum of 4 elements for the flange plate, and a minimum of 2 elements for the lip plate.

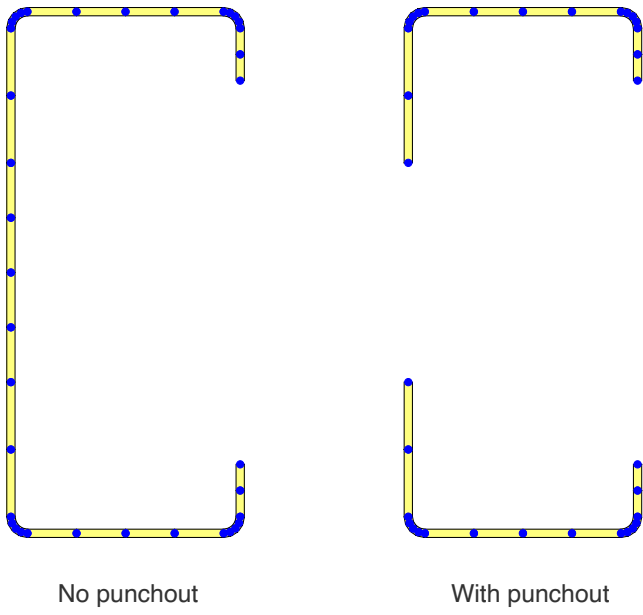


Fig. 2. Finite strip model of lipped channel sections

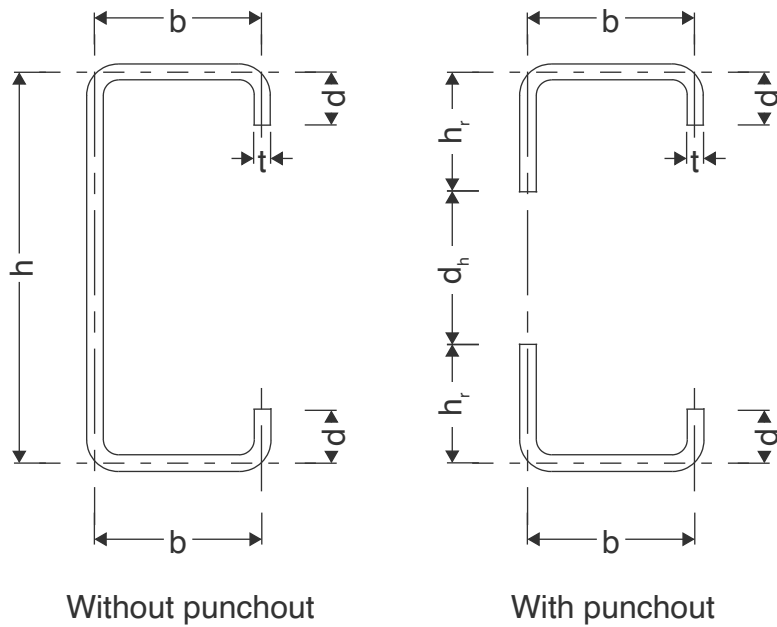


Fig. 3. Centerline dimensions of lipped channel sections

#### 4 Critical buckling local stress from FSM

The critical local buckling mode is identified as the one corresponding to the first local minimum of the signature curve when two local minima exist. When no or only one local minimum is found, the critical

distortional buckling mode may be mistaken as the local one. Therefore, a two-step analysis (Li and Schafer 2010) is used to correctly identify the critical local buckling mode.

The critical buckling loads and moments from the finite strip analysis are converted to the critical local buckling stresses by Eq. (10) and Eq. (11).

$$F_{cr\ell,nh} = \frac{P_{cr\ell,nh}}{A} \quad (10)$$

where  $P_{cr\ell,nh}$  is critical buckling load of the section without hole, and  $A$  is the gross section area.

$$F_{cr\ell,nh} = \frac{M_{cr\ell,nh}}{S_f} \quad (11)$$

where  $M_{cr\ell,nh}$  is critical buckling moment of the section without hole, and  $S_f$  is the gross section modulus with the extreme fiber under compression.

For sections with web punchouts

$$F_{cr\ell,h} = \frac{P_{cr\ell,h}}{A_n} \quad (12)$$

where  $P_{cr\ell,h}$  is critical buckling load of the section with hole, and  $A_n$  is net section area.

$$F_{cr\ell,h} = \frac{M_{cr\ell,h}}{S_{f,n}} \quad (13)$$

where  $M_{cr\ell,h}$  is critical buckling moment of the section with hole, and  $S_{f,n}$  is the net section modulus with the extreme fiber under compression.

## 5 Plate buckling coefficients from FSM

Buckling coefficients  $k$  are not provided by finite strip analyses. Therefore, conversion is required to arrive at the buckling coefficients. By setting the critical buckling stress expression of a plate (Eq. (1)) equal to the section critical buckling stress  $F_{FSM}$  from FSM, the corresponding buckling coefficient of that plate can be determined. This approach applies to all plate elements, including web, flange, lip, and unstiffened web if punchout exists. The conversion is shown in Eq. (14)-(17).

$$F_{FSM} = k_h \frac{\pi^2 E}{12(1 - \mu^2)} \left(\frac{t}{h}\right)^2 \quad (14)$$

$$F_{FSM} = k_b \frac{\pi^2 E}{12(1 - \mu^2)} \left(\frac{t}{b}\right)^2 \quad (15)$$

$$F_{FSM} = k_d \frac{\pi^2 E}{12(1 - \mu^2)} \left(\frac{t}{d}\right)^2 \quad (16)$$

$$F_{FSM} = k_{hr} \frac{\pi^2 E}{12(1 - \mu^2)} \left(\frac{t}{h_r}\right)^2 \quad (17)$$

Note that some care must be taken for sections in bending as the  $F_{FSM}$  must be the critical buckling stress of the compression fiber of the specific plate, which may or may not be at the most extreme fiber of the section.

The buckling coefficients obtained per back-calculation of Eq. (14)-(17) are not traditional isolated plate buckling coefficients given for certain idealized boundary conditions, but instead are specific to lipped channel section geometries and loading conditions. It is possible to develop accurate analytical equations for buckling for these FSM-based buckling coefficients, which can be used to substitute  $k$  in Eq. (1) so that the cross-section critical buckling stress can be conveniently calculated.

For each loading condition, only one buckling coefficient (e.g.,  $k_h$ ) needs to be determined and supporting equations developed. It is a secondary decision to select which plate is used as a reference since an accurate equation can be formulated regardless of the choice. Conceptually, it is easier to develop equations for the buckling coefficient of the plate which typically dominates the section local buckling, e.g., web element for a lipped channel under pure compression. Therefore, in this study, the development of each analytical equation starts with identifying a dominant plate element to focus on, which is done qualitatively by observing buckling mode shapes.

## 6 Sections without punchouts

### 6.1 Pure compression

For pure compression, the web element is typically the dominant plate. The critical local buckling stress is calculated as

$$F_{cr\ell,nh} = k_h \frac{\pi^2 E}{12(1 - \mu^2)} \left(\frac{t}{h}\right)^2 \quad (18)$$

where  $k_h$  is the plate buckling coefficient for the web, and  $h$  is the centerline width of the web.

For a lipped channel section under pure compression, it is found that  $k_h$  is most influenced by the geometric ratio  $h/b$  (Fig. 4). A polynomial ratio expression is used and fit to the FSM data which is obtained by minimizing least-squares error then manually simplified to a condensed and convenient form. The equation developed is Eq. (19)

$$k_h = 4 + \frac{24\eta_h}{20 + 4.4\eta_h + \eta_h^2} \quad (19)$$

where  $\eta_h = h/b$ , and  $1.2 \leq \eta_h \leq 22$

The proposed equation has high prediction accuracy and strong consistency. The mean FSM-to-predicted ratio  $F_{FSM}/F_{pred}$  is 1.00 and COV is 0.02. Fig. 5 shows the distribution of the FSM-to-predicted ratio,  $F_{FSM}/F_{pred}$ . Compared to the results of the element method of AISI S100 (2020) Appendix 2 (as shown in Fig. 5) the proposed equation is more accurate and has significantly less scatter.

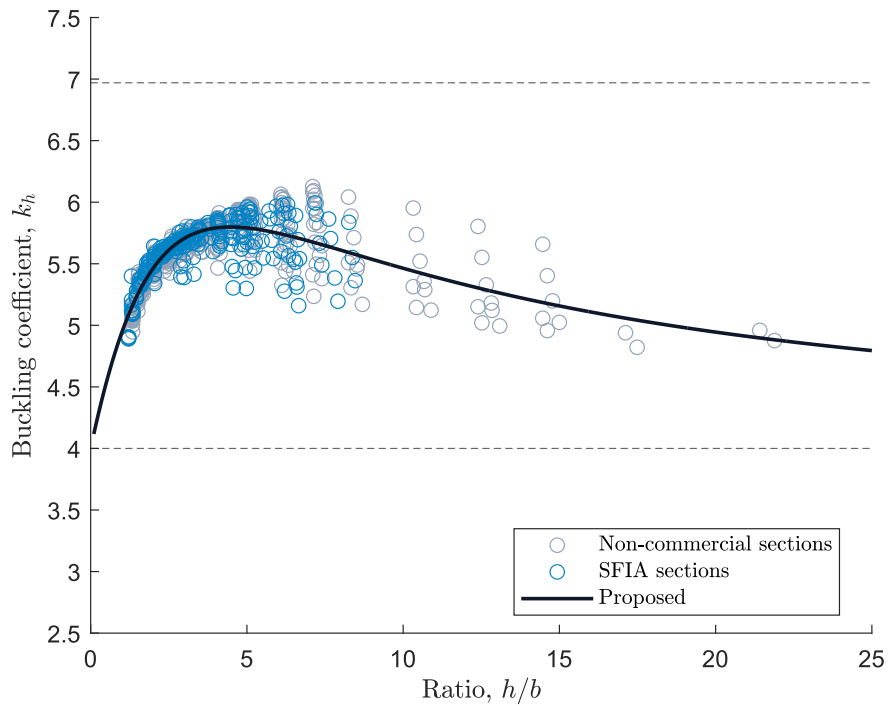


Fig. 4. The proposed equation for gross lipped channel sections under pure compression against FSM results

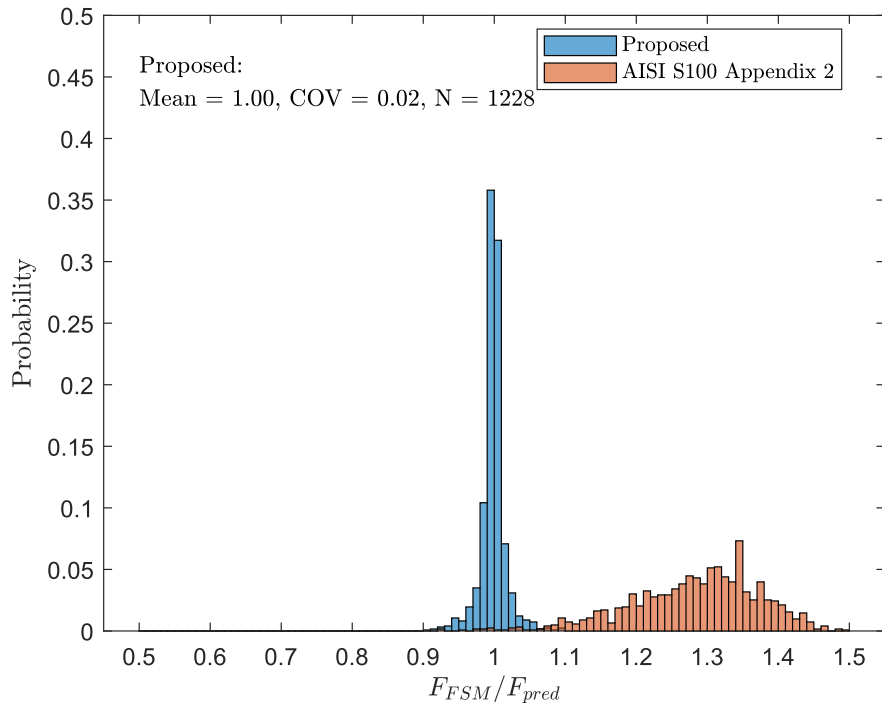


Fig. 5. Histogram of the prediction accuracy of the proposed equation for gross lipped channel section under pure compression

## 6.2 Major axis bending

For a lipped channel section under major axis bending, either the flange or web could be the dominant plate. It is decided to develop analytical equations for each case. For simplicity, a section is considered flange buckling dominant, when the FSM-determined flange plate buckling coefficient  $k_{b,FSM}$  is less than 4; otherwise, the section is considered web buckling dominant. For the FSM data, this division approach can be approximated by  $h/b < 2.57$  for flange buckling dominant and  $h/b \geq 2.57$  for web buckling dominant.

Two analytical equations are developed, Eq. (20) and (22). It is found that both  $k_b$  and  $k_h$  are strongly influenced by the ratio  $h/b$  (Fig. 6). The equations are thusly developed with the ratio  $h/b$  as the single input parameter.

When  $1 < \eta_h < 2.57$

$$F_{cr\ell,nh} = k_b \frac{\pi^2 E}{12(1 - \mu^2)} \left(\frac{t}{b}\right)^2 \quad (20)$$

$$k_b = \frac{4.93 - 3.15\eta_h + 0.53\eta_h^2}{1 - 0.64\eta_h + 0.11\eta_h^2} \quad (21)$$

where  $\eta_h = h/b$

When  $\eta_h \geq 2.57$

$$F_{cr\ell,nh} = k_h \frac{\pi^2 E}{12(1 - \mu^2)} \left(\frac{t}{h}\right)^2 \quad (22)$$

$$k_h = \frac{-4.3\eta_h + 6.44\eta_h^2}{1 - 0.54\eta_h + 0.24\eta_h^2} \quad (23)$$

where  $\eta_h = h/b$ , and  $1.2 \leq \eta_h \leq 22$

The proposed equation has excellent prediction accuracy. The mean of the FSM-to-predicted ratio is 1.00 and COV is 0.03. The histogram of the FSM-to-predicted ratios is shown in Fig. 7. The proposed equation outperforms the element method in AISI S100 Appendix 2 in both accuracy and consistency.

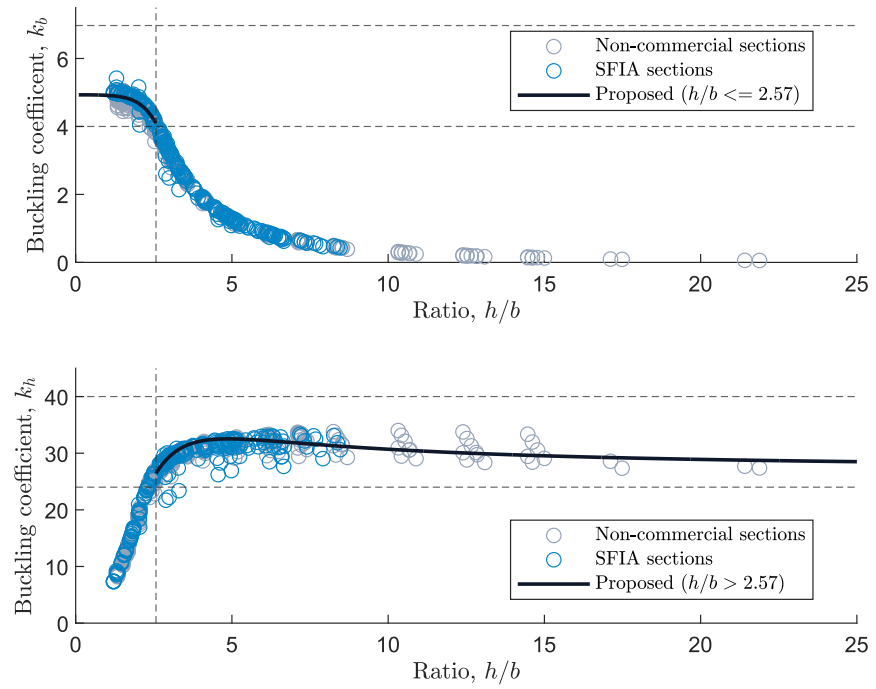


Fig. 6. The proposed equation for gross lipped channel sections under major axis bending against FSM results

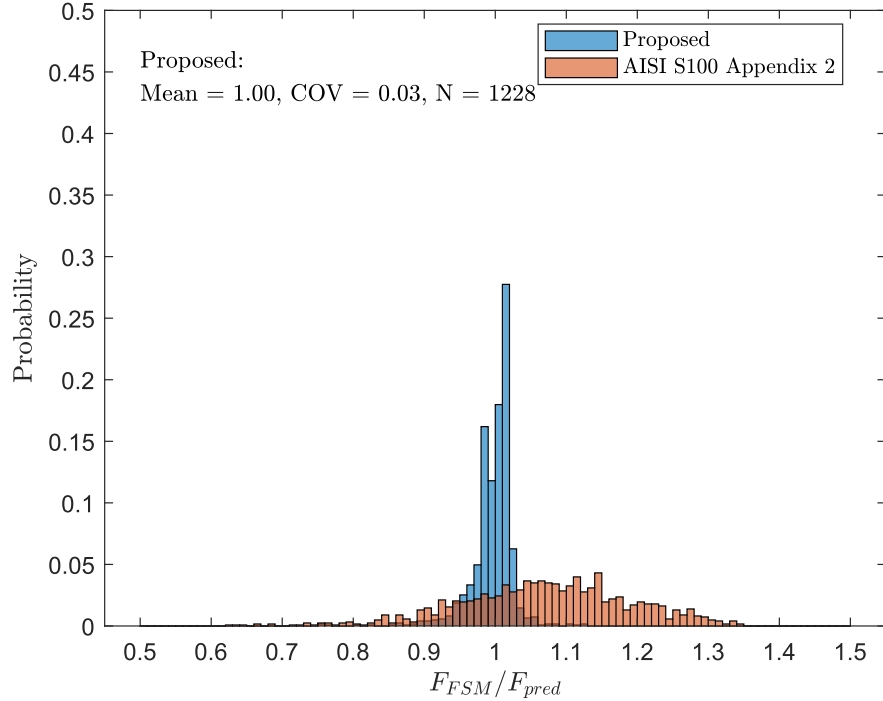


Fig. 7. Histogram of the prediction accuracy of the proposed equation for gross lipped channel section under major axis bending

### 6.3 Minor axis bending with lip in compression

For lipped channel sections under minor axis bending with the lip in compression, the dominant plate is found to be the flange. The plate buckling coefficient  $k_b$  is found to be dependent on both the geometric ratio  $b/d$  and the stress gradient  $\psi$  (Fig. 8), where  $\psi = |f_2/f_1|$  (see AISI S100 for definitions of  $f_1$  and  $f_2$ ).  $k_b$  increases with higher  $b/d$  until reaching a plateau at  $b/d$  around 5; at the same  $b/d$  values, higher  $\psi$  leads to larger  $k_b$ .

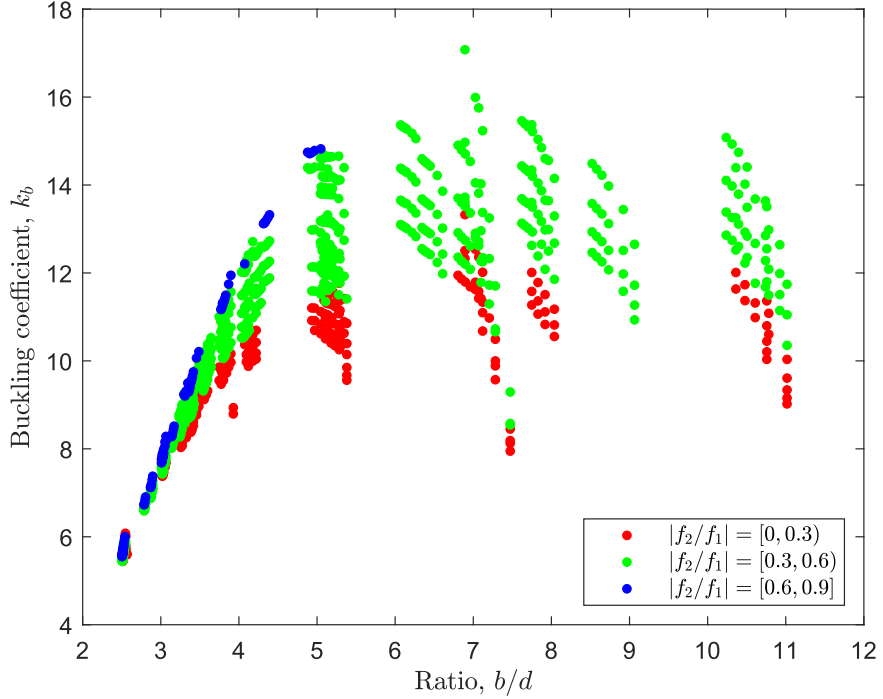


Fig. 8. Dependency of the buckling coefficient of minor-axis bending with lip in compression on geometric ratio and stress gradient

It is decided to explicitly include both the effect of  $k_b$  and  $\psi$  in the proposed analytical equation. Specifically, the equation is split into two parts,  $f(\cdot)$  and  $g(\cdot)$ , as seen in Eq. (24). The first part considers the contribution of the stress gradient  $\psi$ , and the second part considers the contribution of the geometric ratio  $b/d$ .

$$k_b = f(\psi, \dots) + g(b/d, \dots) \quad (24)$$

The part  $f(\cdot)$  is first determined. Fig. 9 shows the relationship between the buckling coefficient  $k_b$  and stress gradient  $\psi$  at various  $b/d$  ratios. Several conclusions can be drawn from Fig. 9. First, at a given  $b/d$  ratio, the relationship between buckling coefficient and stress gradient is approximately linear. Second, the magnitude of the stress gradient effect is also dependent on the ratio of  $b/d$ . Based on these findings,  $f(\cdot)$  can be established as  $\xi(b/d)\psi$ , where  $\xi$  is a stress gradient multiplier dependent on  $b/d$ .

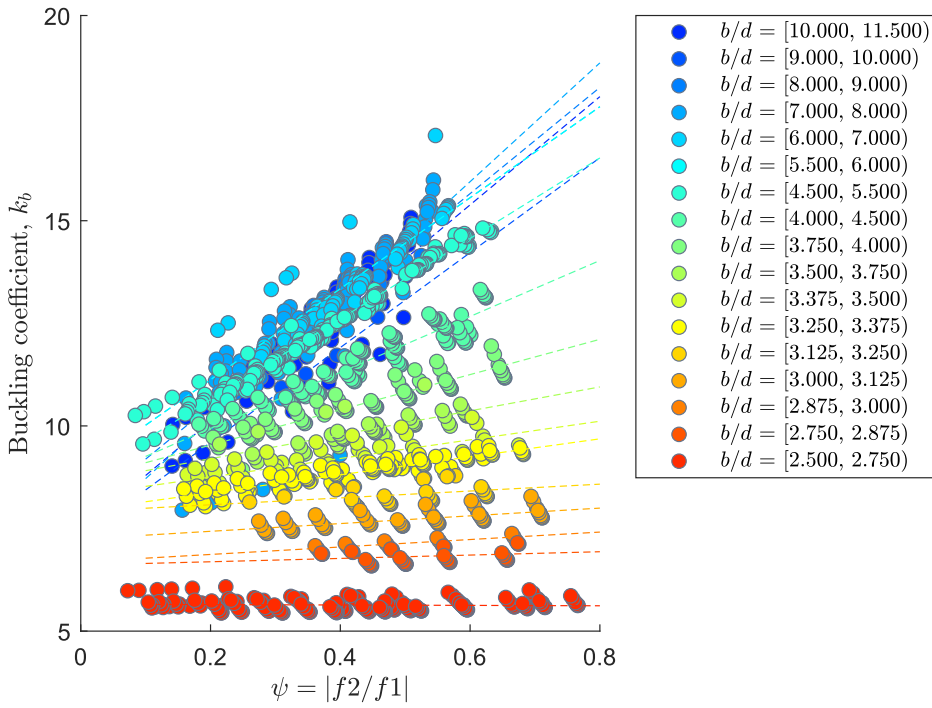


Fig. 9. Comparisons between the relationship between buckling coefficient and stress gradient at different geometric ratios for lipped channel sections under minor axis bending with lip in compression

The expression for the stress gradient multiplier  $\xi$  is determined empirically.  $\xi$  is calculated for each group of FSM data with similar  $b/d$  ratios (difference less than 0.125).  $\xi$  is plotted as against  $b/d$  in Fig. 10. Each data point corresponds to a stress gradient multiplier specific to a  $b/d$  ratio. A linear expression with upper and lower limits can be developed for  $\xi$  as shown in Eq. (25).

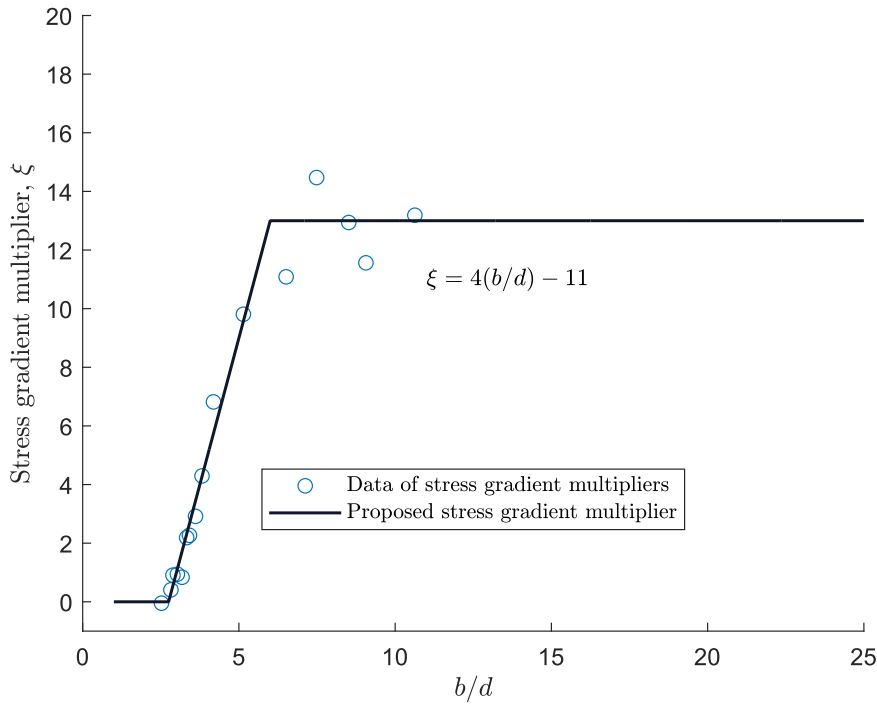


Fig. 10. Stress gradient multiplier against geometric ratio for lipped channel sections under minor axis bending with lip in compression

$$\xi = 4\eta_b - 11 \quad (25)$$

where  $\eta_b = b/d$ , and  $0 \leq \xi \leq 13$

Therefore,  $f(\cdot)$  can be determined as

$$f(\cdot) = \xi\psi = \begin{cases} 0 & \eta_b \leq 2.75 \\ (4\eta_b - 11)\psi & 2.75 < \eta_b \leq 6 \\ 13\psi & \eta_b > 6 \end{cases} \quad (26)$$

The part  $g(\cdot)$  can be determined accordingly by removing part  $f(\cdot)$  from  $k_b$ . The relation between  $k_b - \xi\psi$  and  $b/d$  ratio is shown in Fig. 11. A polynomial ratio expression is used to fit to the data.

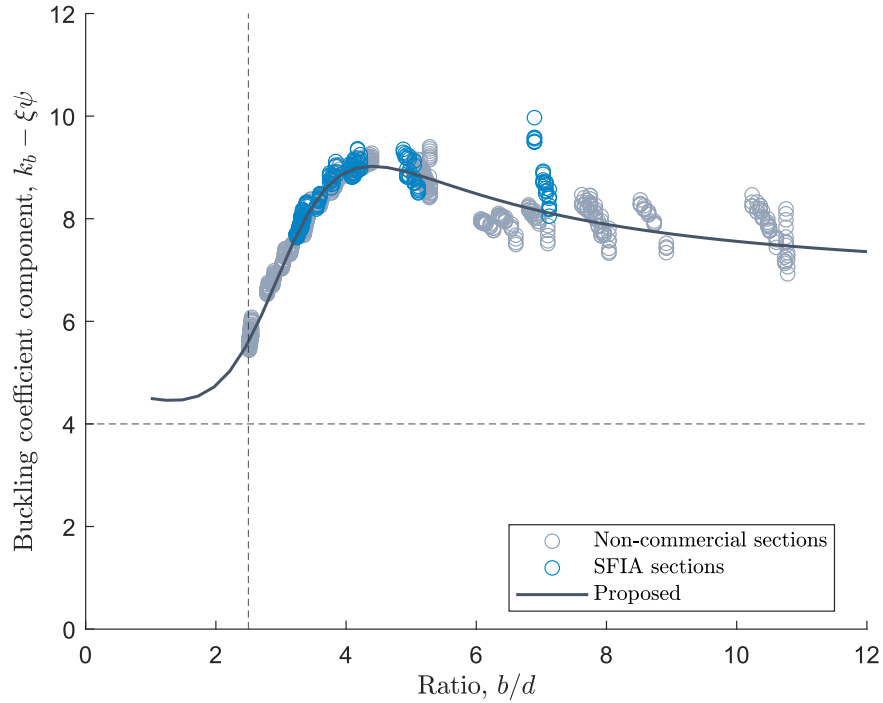


Fig. 11. The proposed equation for gross lipped channel sections under minor axis bending with lip in compression against FSM results

$$g(\cdot) = 4 + \frac{0.8 - 0.758\eta_b + 0.234\eta_b^2}{1 - 0.533\eta_b + 0.09\eta_b^2} \quad (27)$$

where  $\eta_b = b/d$ , and  $2.5 \leq \eta_b \leq 11.1$

Adding the two parts together, the full equation can be expressed as shown in Eq. (28) along with supporting equations Eq. (29) - (30). Fig. 12 shows the histogram of the FSM-to-predicted ratios. The proposed equation is highly accurate (mean = 1.00) and has low variation (COV = 0.02). Compared to element method in AISI S100 Appendix 2, the proposed equation has significantly better performance. Note that for AISI element method, the centerline lip dimension is used for all sections to mitigate the reduced accuracy due to larger corner radius.

$$k_b = k_{b1} + k_{b2} \quad (28)$$

$$k_{b1} = 4 + \frac{0.8 - 0.758\eta_b + 0.234\eta_b^2}{1 - 0.533\eta_b + 0.09\eta_b^2} \quad (29)$$

$$k_{b2} = \begin{cases} 0 & \eta_b \leq 2.75 \\ (4\eta_b - 11)\psi & 2.75 < \eta_b \leq 6 \\ 13\psi & \eta_b > 6 \end{cases} \quad (30)$$

where  $\eta_b = b/d$  ( $2.5 \leq \eta_b \leq 11.1$ ),  $\psi = |f_2/f_1|$  ( $0.07 \leq \psi \leq 0.77$ )

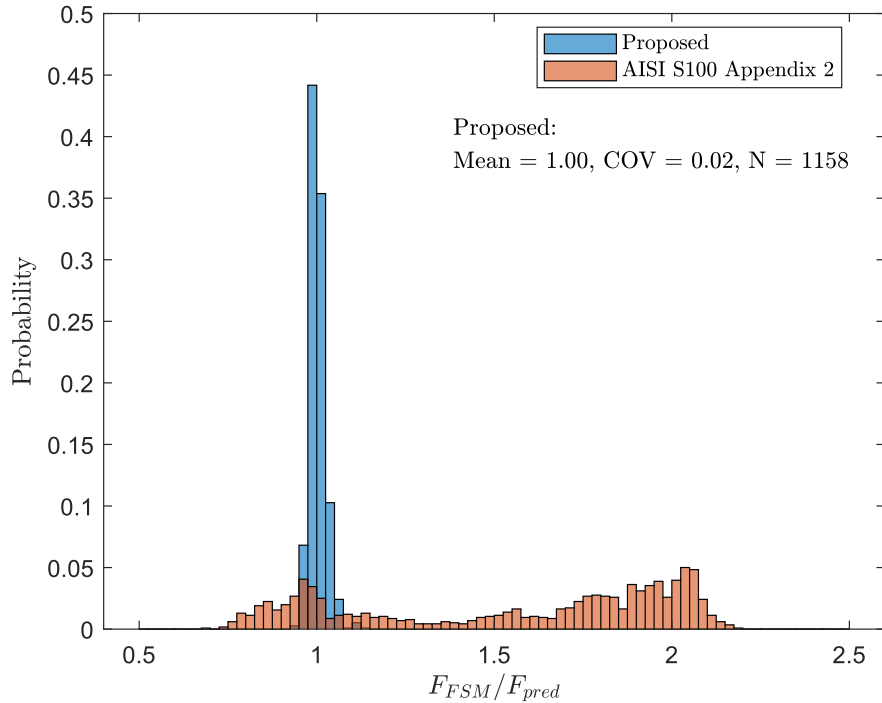


Fig. 12. Histogram of the prediction accuracy of the proposed equation for gross lipped channel section under minor axis bending with lip in compression

It is worth noting that a small set of FSM results with  $d/t < 4.4$  are excluded from the curve fitting. The buckling stresses of these data are unusually lower than comparable sections with greater  $d/t$  ratios. Through observation of the buckling mode shapes, it is found that the buckling modes of these FSM results consist of a considerable amount of distortional buckling, which are represented by displacement of flange-web junctures. The use of the proposed equation Eq. (28) shall be subject to the sections with slender lips, specifically  $d/t \geq 4.4$ .

#### 6.4 Minor axis bending with lip in tension

For lipped channel sections under minor axis bending with the lip in tension, the web is under uniform compression and flange is under stress gradient. The section-level buckling is dominated by web buckling. In Fig. 13, the web buckling coefficient  $k_h$  is plotted against the ratio of  $h/b$  for all FSM results. A polynomial ratio expression is fit to the FSM data. The proposed equation is expressed in Eq. (31). The histogram of the FSM-to-predicted ratios by the proposed equation is shown in Fig. 14. For the proposed equation, the mean FSM-to-predicted ratio is 1.00 and COV = 0.02. In comparison to the element method in AISI S100 Appendix 2 equations, the proposed equation is more accurate and has lower variations.

$$k_h = 4 + \frac{1.36 - 0.014\eta_h}{1 - 0.12\eta_h + 0.012\eta_h^2} \quad (31)$$

where  $\eta_h = h/b$ , and  $1.2 \leq \eta_h \leq 22$

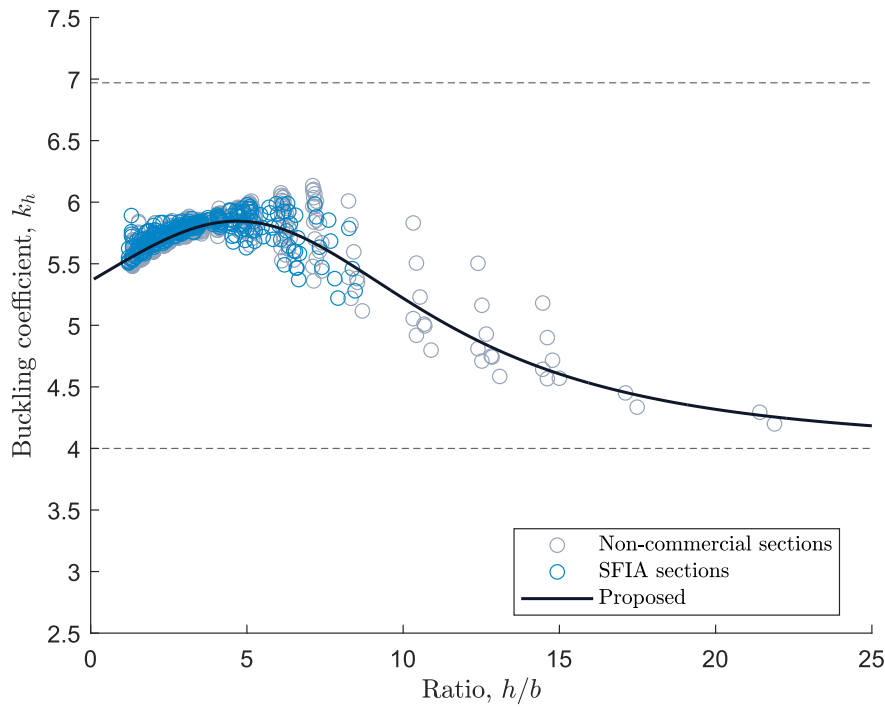


Fig. 13. The proposed equation for gross lipped channel sections under minor axis bending with lip in tension against FSI results

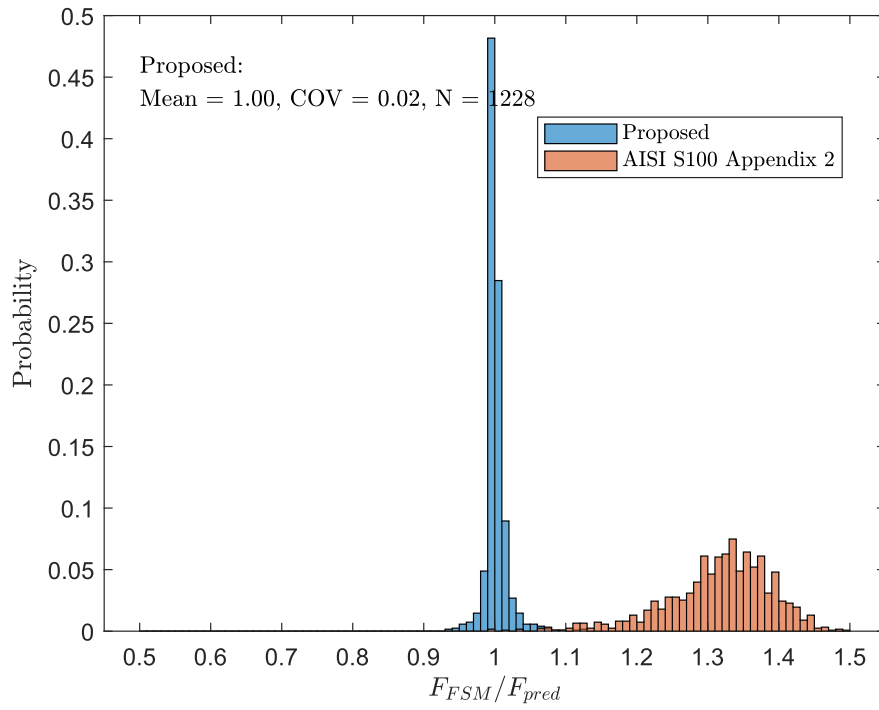


Fig. 14. Histogram of the prediction accuracy of the proposed equation for gross lipped channel section under minor axis bending with lip in tension

## 7 Sections with standard web punchouts

### 7.1 Determine critical local buckling load/moment

Web punchouts are used ubiquitously in cold-formed steel framing to allow for service such as electrical wiring or plumbing as well as to provide bridging to brace studs. Depending on the length and width, the presence of a punchout in the web may reduce the critical local buckling load or moment of the section. For a lipped channel with a web punchout, the web has two conditions with respect to plate buckling: within the punchout region, the web is essentially an unstiffened element; while outside the punchout region, the web is a stiffened element, supported by the two flanges.

The Appendix 2 Commentary in AISI S100 (2020) recommends taking the minimum of the critical buckling loads under the two conditions as the actual critical load. For compression, this is expressed as Eq. (32). For bending, this is expressed as Eq. (33).

$$P_{cr\ell} = \min(P_{cr\ell,nh}, P_{cr\ell,h}) \quad (32)$$

where  $P_{cr\ell,h}$  is the critical buckling load of the section without punchout, and  $P_{cr\ell,nh}$  is the critical buckling load of the section with punchout and buckling half wavelength shorter than the punchout length.

$$M_{cr\ell} = \min(M_{cr\ell,nh}, M_{cr\ell,h}) \quad (33)$$

where  $M_{cr\ell,h}$  is the critical buckling moment of the section without punchout, and  $M_{cr\ell,nh}$  is the critical buckling moment of the section with punchout and buckling half wavelength shorter than the punchout length.

Accurate analytical equations have been proposed for calculating  $P_{cr\ell,nh}$  and  $M_{cr\ell,nh}$  in the previous section. This section focuses on developing analytical equations for calculating  $P_{cr\ell,h}$  and  $M_{cr\ell,h}$  from FSM analysis.

In this study, only standard SFIA punchout sizes are considered and the dimensions are shown in Fig. 15. Specifically, the punchout width is 0.75 in. for sections not deeper than 2.5 in. and 1.5 in. for the rest. The punchout length is 4 in. for all sections.

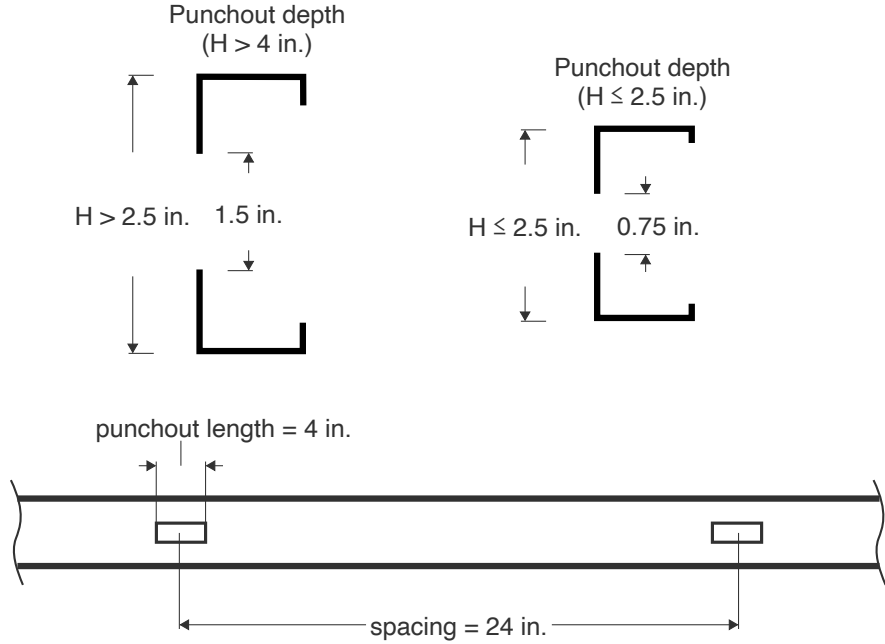


Fig. 15. Dimensions of standard web punchout

## 8 Determine critical local buckling stress

FSM analysis is conducted for the same 1228 lipped channel sections in the no-punchout study but with the web punchout modeled. After the critical buckling loads or moments are determined, the critical buckling stresses are calculated using net section properties as detailed in Eq. (12) and (13).

Different from the no-punchout study, there is an extra step in determining the  $F_{cr\ell}$  for sections with punchouts. It is required that the buckling half-wavelength of the  $F_{cr\ell}$  shall not be greater than the punchout length. In other words, the critical local buckling half-wavelengths must be restrained. For sections with the “unrestrained” buckling half wavelength great than the punchout length, the  $F_{cr\ell}$  must be taken as the value of the mode with half wavelength equal to the punchout length. When this occurs, the final  $F_{cr\ell}$  are usually higher than the “unrestrained” values. This approximation was developed by Moen and Schafer (2009) and shown to agree well with more advanced shell finite element models.

For developing the analytical expressions, the effect of half buckling wavelength restraint is considered separately as shown in Eq. (34), where this effect is represented by a multiplier  $C_L$  over the unrestrained critical buckling stress  $F_{cr\ell 0}$ . The value of  $C_L$  is set to be always greater or equal to 1.0.

$$F_{cr\ell,h} = C_L F_{cr\ell 0} \quad (34)$$

where  $C_L$  is half wavelength restraint multiplier and  $F_{cr\ell 0}$  is the unrestrained critical buckling stress

$C_L$  is determined from FSM analysis as follows. The unrestrained critical local buckling stress is first determined via FSM analysis as  $F_{FSM 0}$ . Then restrained critical local buckling stress  $F_{FSM}$  is then determined by imposing the half-wavelength restraint. With both  $F_{FSM 0}$  and  $F_{FSM}$  determined,  $C_L$  can be calculated by plugging  $F_{FSM 0}$  and  $F_{FSM}$  into Eq. (34).

## 8.1 Pure compression

For pure compression, the net section local buckling stress is calculated by Eq. (35).

$$F_{cr\ell,h} = C_L k_{hr0} \frac{\pi^2 E}{12(1 - \nu^2)} \left(\frac{t}{h_r}\right)^2 \quad (35)$$

where  $k_{hr0}$  is the unrestrained buckling coefficient corresponding to the unstiffened web element, and  $h_r$  is the width of the unstiffened web element (see Fig. 3).

Similar to the no-punchout sections, the critical buckling stresses determined from the FSM analysis can be converted to the buckling coefficients of the dominant plate, which is the unstiffened web element for pure compression in this study.

The buckling of the unstiffened web element is mainly affected by the restraint provided by the flange. Therefore, the relationship between the buckling coefficient  $k_{hr0}$  and the geometric ratio  $b/h_r$  is explored. As shown in Fig. 16,  $k_{hr0}$  is closely dependent on  $b/h_r$ , when  $b/h_r$  is larger than 0.75. When  $b/h_r$  is below 0.3, there is a moderate scatter among FSM data points, primarily driven by non-commercial sections with small flanges ( $b/h$  below 0.15) not typically used practice. An analytical equation is proposed in Eq. (36).

$$k_{hr0} = \frac{1.02}{1 + 0.04\eta_{hr}^3} \geq 0.43 \quad (36)$$

where  $\eta_{hr} = b/h_r$ , and  $0.1 \leq \eta_{hr} \leq 3$

For considering the restraint on buckling half wavelength, an equation is also developed for  $C_L$  (Eq. (37)) and compared against the FSM results in Fig. 17.

$$C_L = \frac{0.14 + 0.15p_d}{1 - 0.05p_d} \geq 1 \quad (37)$$

where  $p_d = (d_h/h)^{-1}$

As the AISI element method does not consider the effect of hole length, the proposed equation for the unrestrained  $F_{cr\ell}$  is compared against the element method in Fig. 18. The overall performance of the suite of equations for pure compression can be seen Fig. 19.

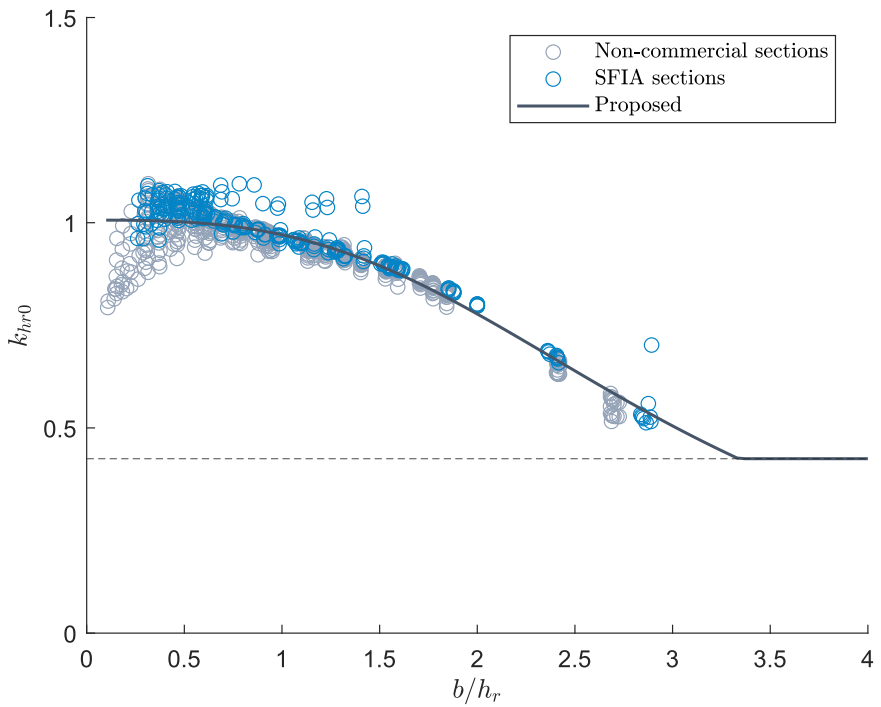


Fig. 16. Comparing the proposed equation for unrestrained buckling coefficients against FSM results for lipped channel sections with punchout under pure compression

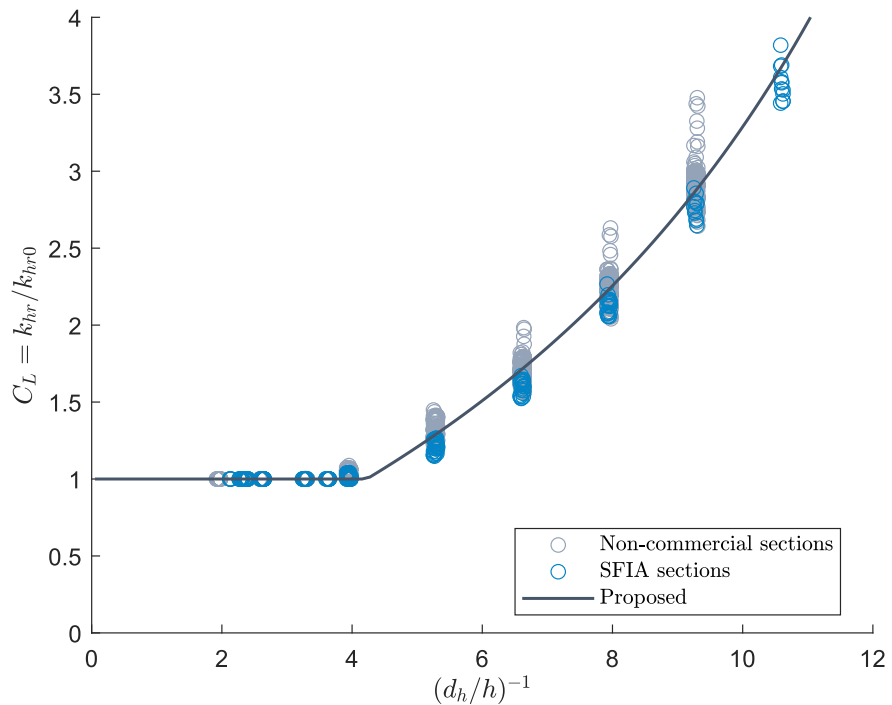


Fig. 17. Comparing the proposed equation for the effect of punchout length restraint against FSM results for lipped channel sections with punchout under pure compression

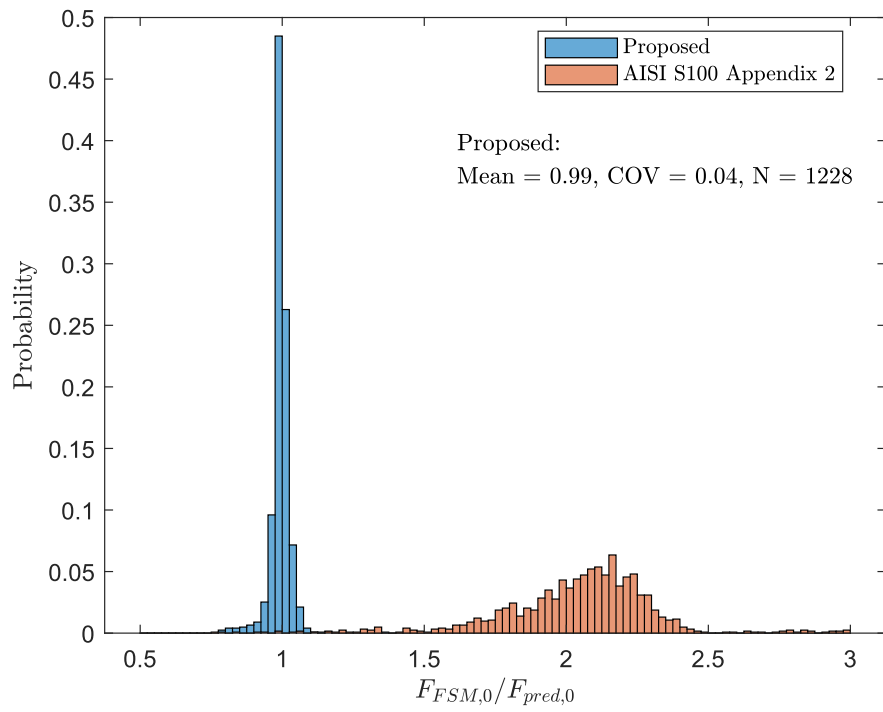


Fig. 18. Histogram of the prediction accuracy of the proposed equation for lipped channel sections with punchouts under pure compression without considering punchout length

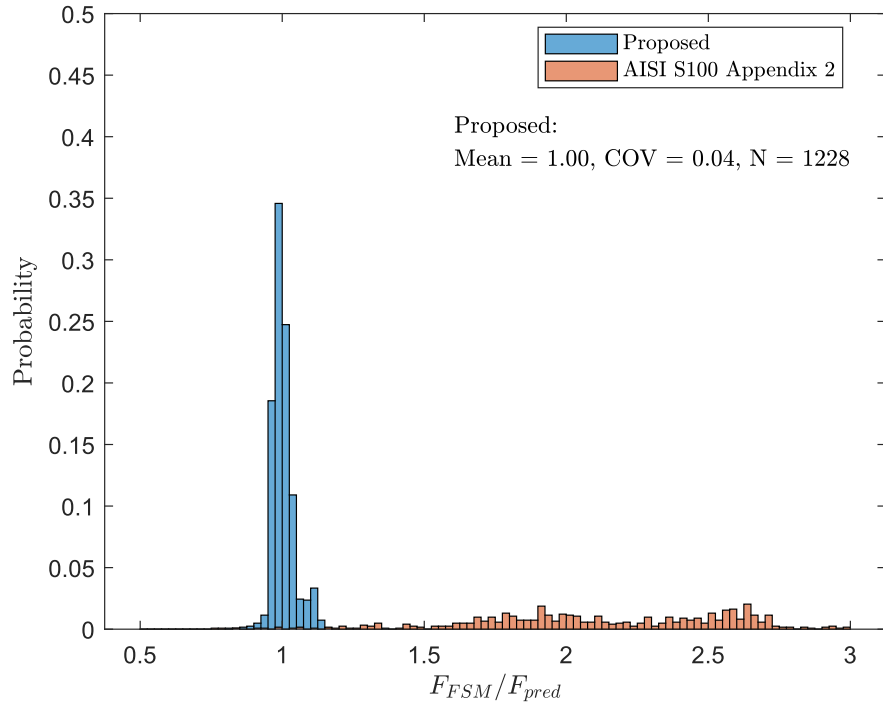


Fig. 19. Histogram of the prediction accuracy of the proposed equation for lipped channel sections with punchouts under pure compression

## 8.2 Major axis bending

For major axis bending, geometric ratio  $b/h_r$  and web stress gradient  $\psi$  are found to be the two main contributing factors to the section's local buckling stress. It is found that the contributions of  $b/h_r$  and  $\psi$  are coupled, which makes it difficult to isolate each contribution for equation development. For convenient consideration of both factors, a surrogate parameter is used instead, specifically  $(b/h_r)(1 - 0.75\psi)$ .

The parameter  $(b/h_r)(1 - 0.75\psi)$  is found to be closely related to  $k_{hr0}$ , which is the unrestrained buckling coefficient of the unstiffened web element (Fig. 20). The analytical equation for  $k_{hr0}$  is developed with  $(b/h_r)(1 - 0.75\psi)$  as the single input variable as shown in Eq. (39) and (40). The proposed equation follows the FSM data well.

A similar surrogate parameter approach is also applied to the development of equation for the multiplier  $C_L$ . The parameter chosen for the development is  $(h - 0.3b - 0.3d)/(h - 2h_r)$ , which considers the effects of  $b/(h - 2h_r)$  and  $d/(h - 2h_r)$  ratios in addition to the ratio  $h/(h - 2h_r)$ . The analytical equation developed for  $C_L$  is expressed as Eq. (41).

The performance of the proposed equation for the unrestrained  $F_{cr\ell}$  is compared against the element method in Fig. 22. The overall accuracy of the proposed equations for major axis bending is shown in Fig. 23.

$$F_{cr\ell,h} = C_L k_{b0} \frac{\pi^2 E}{12(1 - \nu^2)} \left(\frac{t}{b}\right)^2 \quad (38)$$

When  $\eta_{hrp} < 0.298$

$$k_{b0} = \frac{2.952\eta_{hrp}^2}{1 - 2.142\eta_{hrp}^2} \quad (39)$$

When  $\eta_{hrp} \geq 0.298$

$$k_{b0} = \frac{0.152 + 6.974\eta_{hrp}^3}{1 + 1.277\eta_{hrp}^3} \quad (40)$$

where  $\eta_{hrp} = (b/h_r)(1 - 0.75\psi)$ ,  $0.1 \leq \eta_{hrp} \leq 2$ , and  $0.09 \leq \psi \leq 0.52$

$$C_L = \frac{0.502 + 0.093p_d^*}{1 - 0.055p_d^*} \geq 1 \quad (41)$$

where  $p_d^* = (d_h/(h - 0.3b - 0.3d))^{-1}$

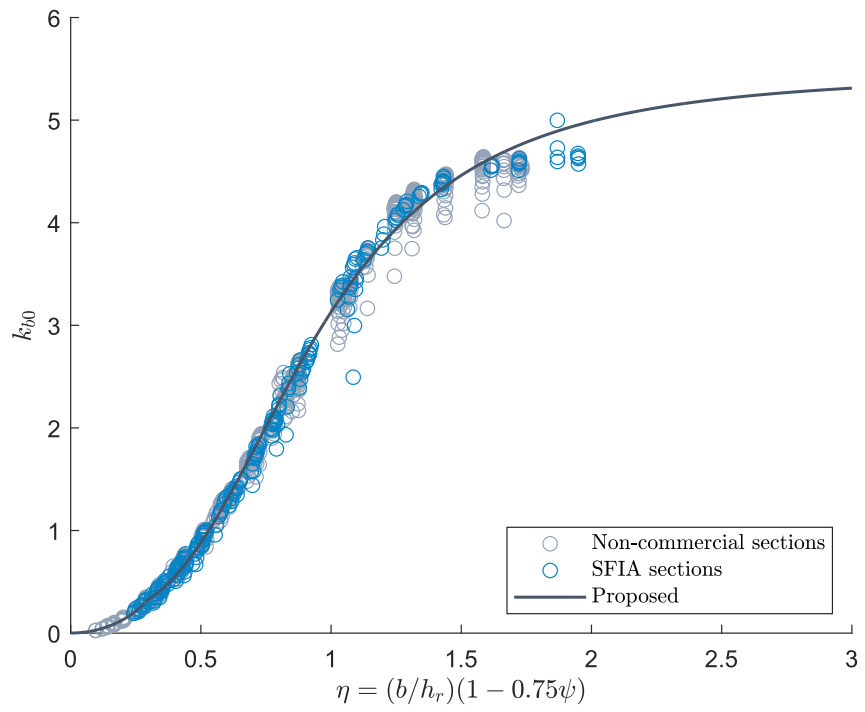


Fig. 20. Comparing the proposed equation for unrestrained buckling coefficients against FSM results for lipped channel section with punchout under major axis bending

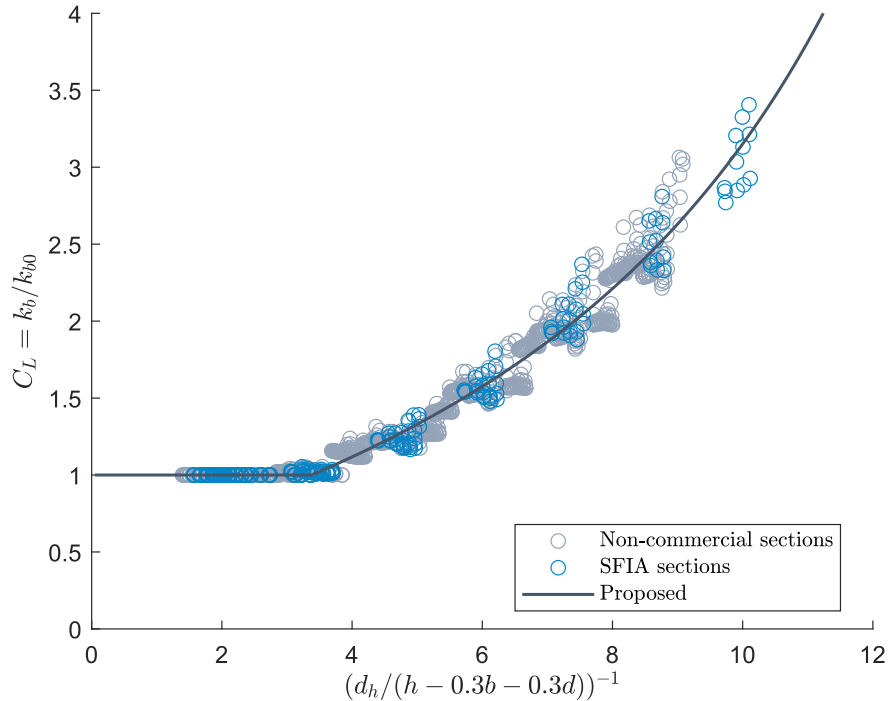


Fig. 21. Comparing the proposed equation for the effect of punchout length restraint against FSM results for lipped channel section with punchout under major axis bending

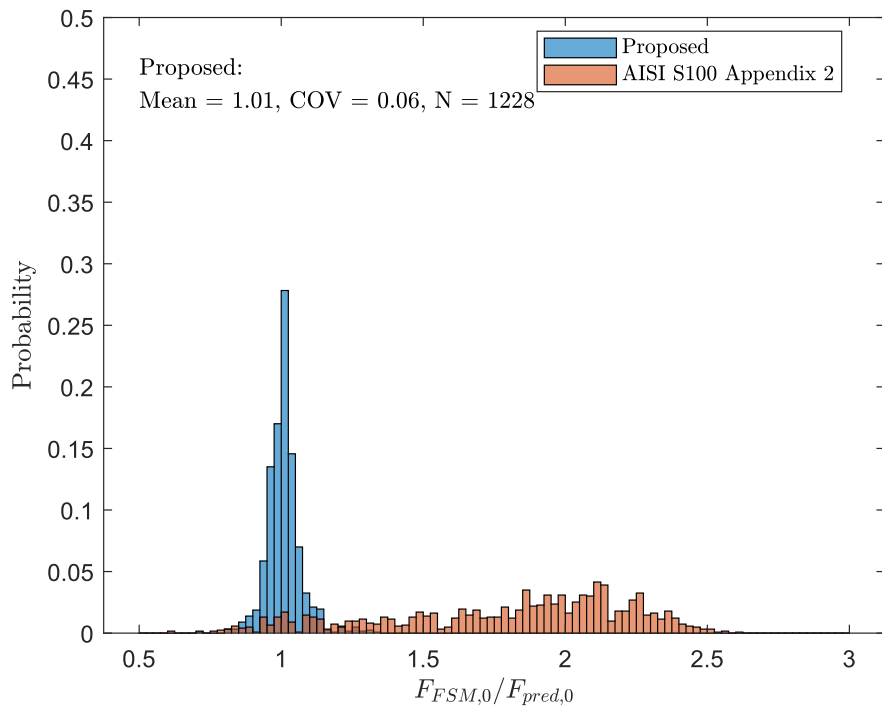


Fig. 22. Histogram of the prediction accuracy of the proposed equation for lipped channel sections with punchouts under major axis bending without considering punchout length

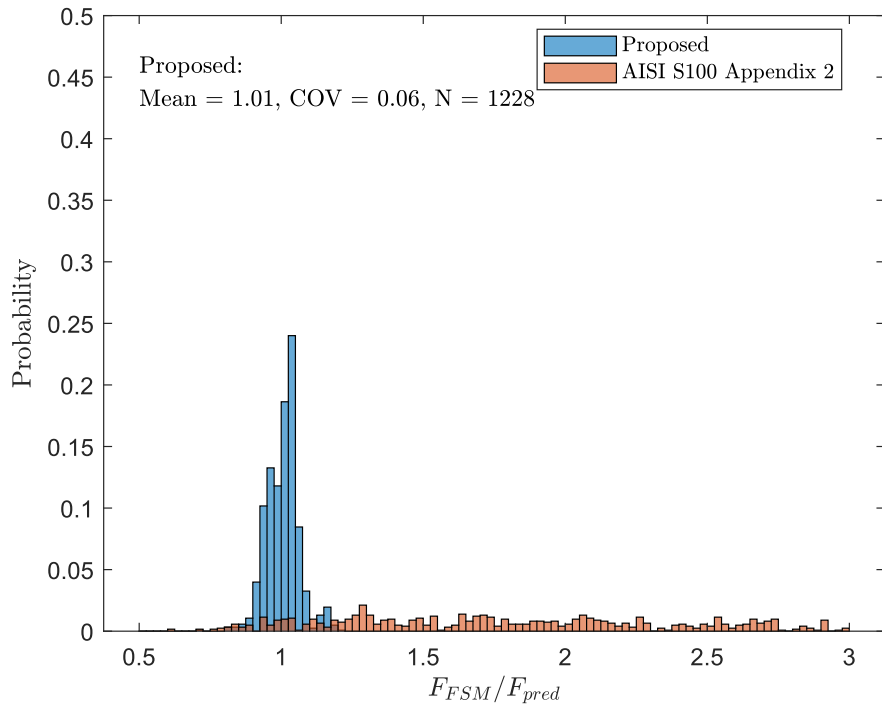


Fig. 23. Histogram of the prediction accuracy of the proposed equation for lipped channel sections with punchouts under major axis bending

### 8.3 Minor axis bending with lip in compression

Under minor axis bending with the lip in compression, the lipped channel sections with punchouts are similar to the ones without punchouts from a plate buckling standpoint, because the web portions are in tension in both cases, and as a result there is no need to consider web punchout length. Therefore, the suite of equations developed for sections without web punchouts namely Eq. (28) are directly applicable to the corresponding sections with web punchouts. However, note that stress gradient and section properties must be calculated for the net section because the presence of the hole will change the neutral axis position and section properties. Similar to the sections without holes, the centerline lip dimension is used for the element method. The performances of Eq. (28) – (30) on the sections without web punchouts are shown in Fig. 24. It is found that Eq. (28) perform well for the cases with web punchouts.

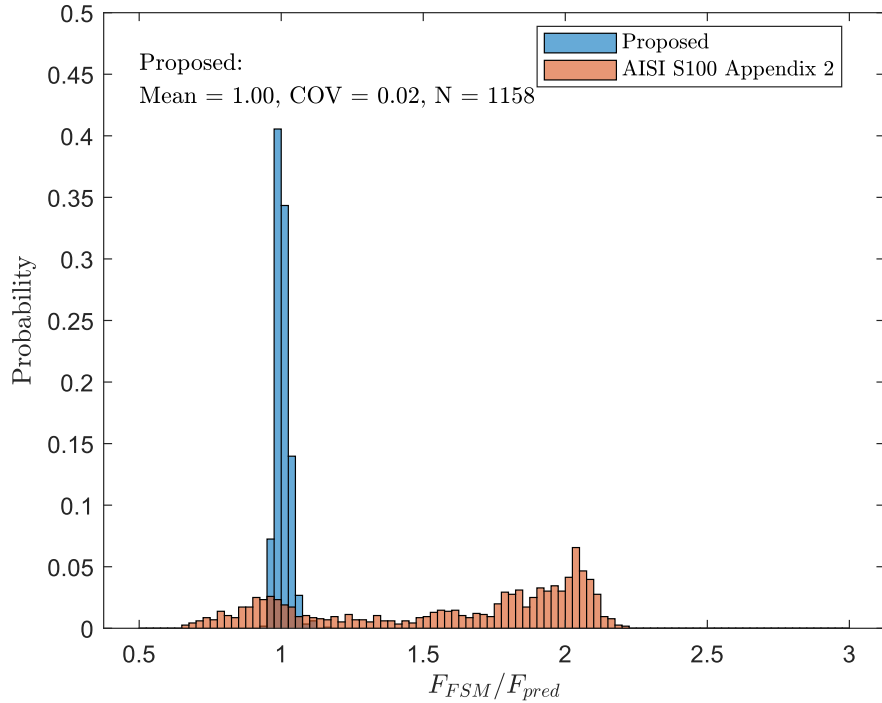


Fig. 24. Histogram of the prediction accuracy of the proposed equation for lipped channel sections with punchouts under minor axis bending with lip in compression

### 8.4 Minor axis bending with lip in tension

The unstiffened web element is the dominant plate in the local buckling of a lipped channel section under minor axis bending with the lip in tension. The critical local buckling stress is thusly calculated by Eq. (35). The unrestrained buckling coefficient  $k_{hr0}$  is found be closely dependent on the ratio of  $b/h_r$  as shown in Fig. 25. When  $b/h_r$  is smaller than 0.4, the deeper flange increases  $k_{hr0}$  by providing stronger restraint for the unstiffened web element. When  $b/h_r$  is greater than 0.4, the larger  $b/h_r$  leads to decrease in the section local buckling strength, because the flange becomes slenderer.

An analytical equation for  $k_{hr0}$  is developed as shown in Eq. (42) and (43). The effect of punchout length restraint is considered by the multiplier  $C_L$ . The analytical equation for  $C_L$  is developed as Eq. (44). The

accuracy of the proposed equation for the unrestrained  $F_{cr\ell}$  is compared with that of the element method in Fig. 27. The final performance of the suite equations is shown in Fig. 28.

When  $\eta_{hr} < 0.4$

$$k_{hr0} = \frac{1.15\eta_{hr}}{0.05 + \eta_{hr}} \quad (42)$$

When  $\eta_{hr} \geq 0.4$

$$k_{hr0} = 1.04 - 0.04\eta_{hr} \quad (43)$$

where  $\eta_{hr} = b/h_r$ , and  $0.1 \leq \eta_{hr} \leq 3$

$$C_L = \frac{0.11 + 0.15p_d}{1 - 0.05p_d} \geq 1 \quad (44)$$

where  $p_d = (d_h/h)^{-1}$

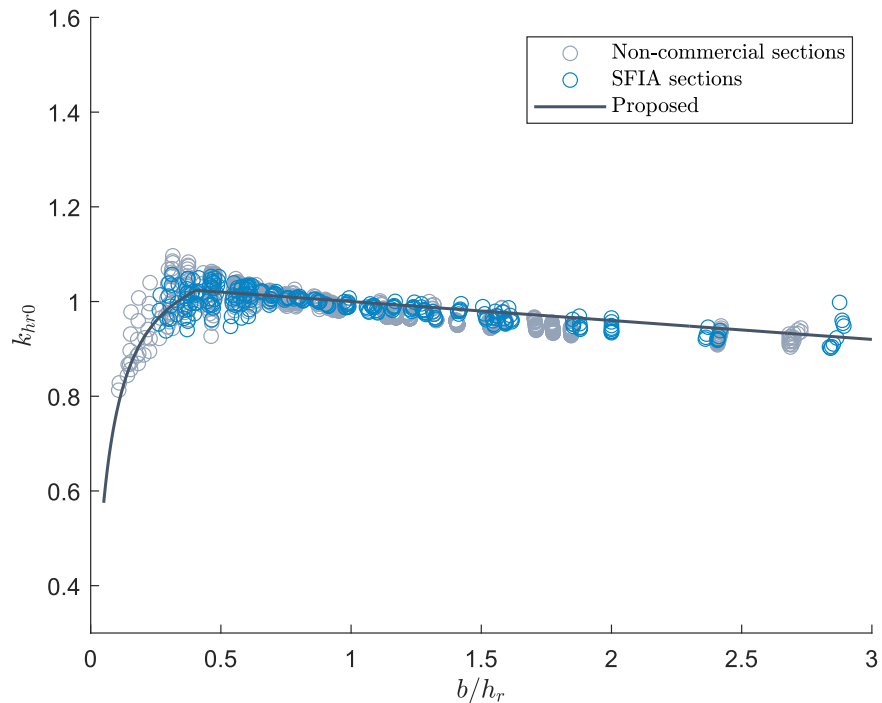


Fig. 25. Comparing the proposed equation for unrestrained buckling coefficients against FSM results for lipped channel section with punchout under minor axis bending with lip in tension

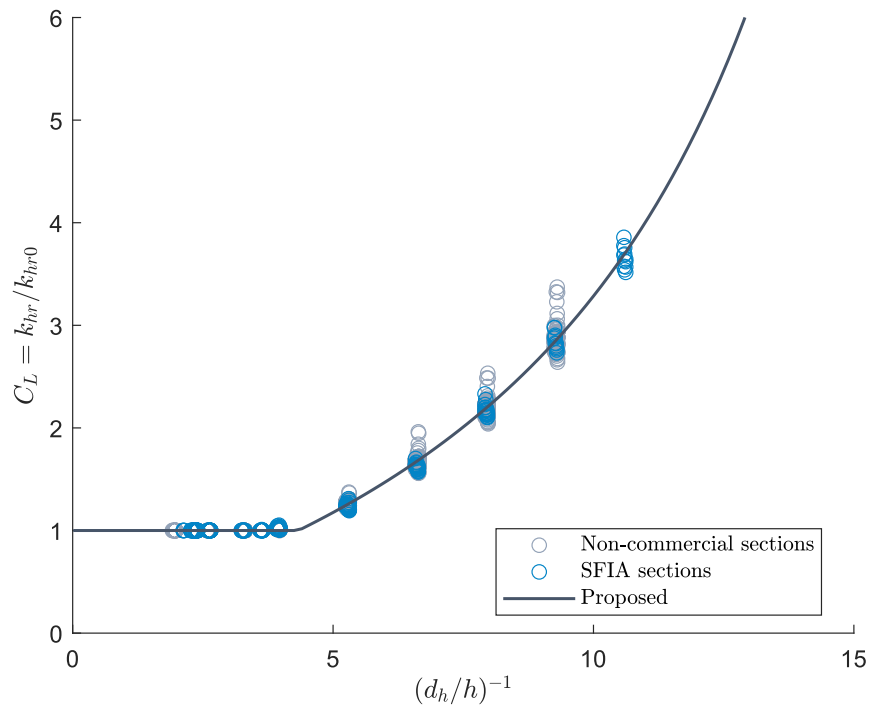


Fig. 26. Comparing the proposed equation for the effect of punchout length restraint against FSM results for lipped channel sections with punchout under minor axis bending in tension

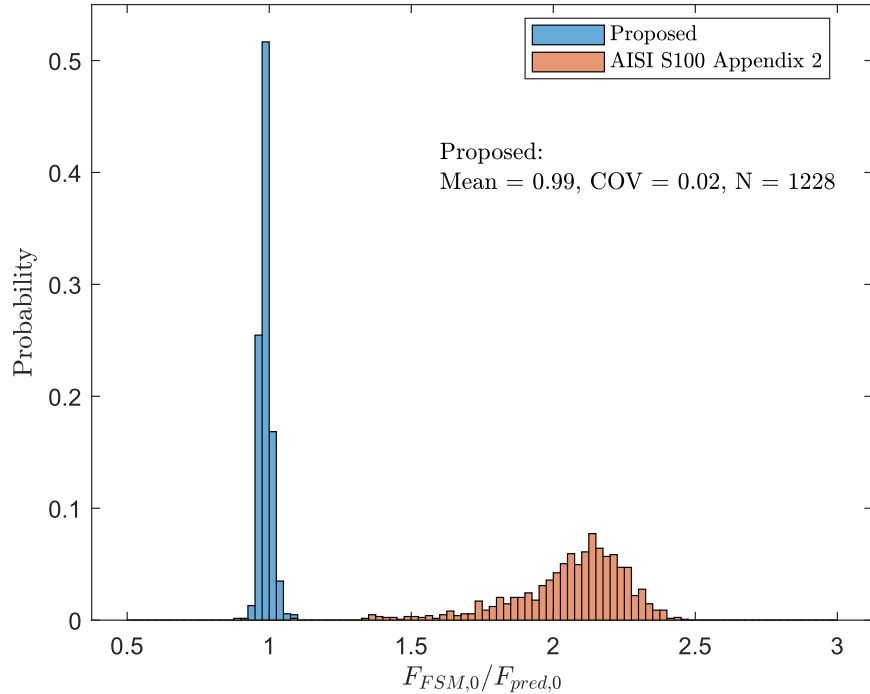


Fig. 27. Histogram of the prediction accuracy of the proposed equation for lipped channel sections with punchouts under minor axis bending with lip in tension without considering punchout length

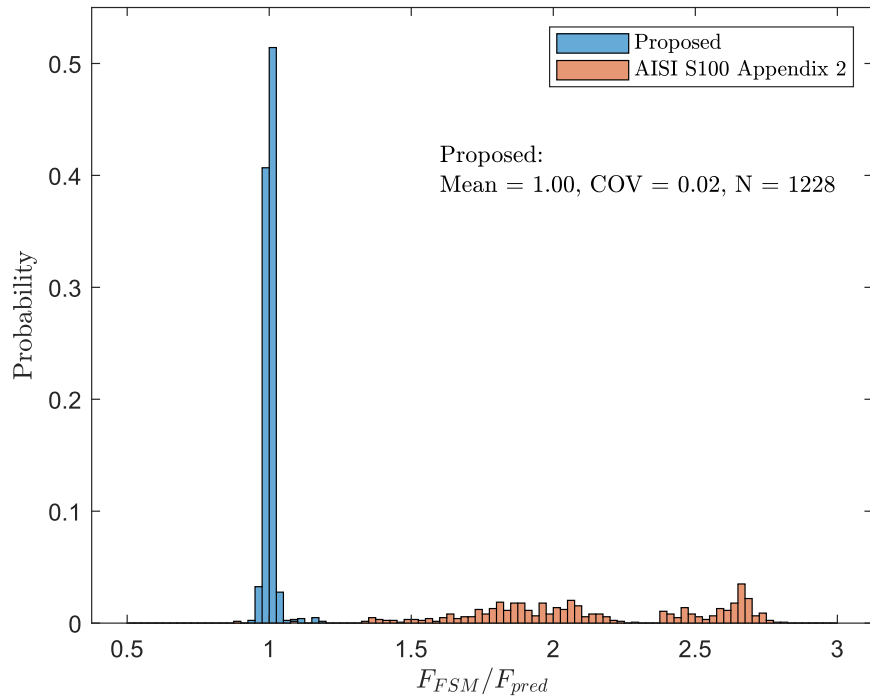


Fig. 28. Histogram of the prediction accuracy of the proposed equation for lipped channel sections with punchouts under minor axis bending with lip in tension

## 9 Summary of performance of proposed equations

Table 1. Summary of the performance of the proposed equations for sections without holes

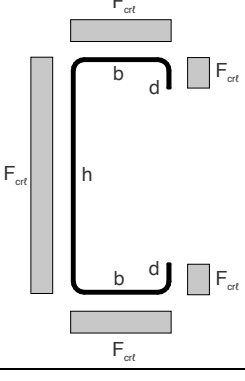
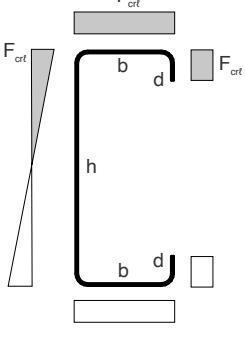
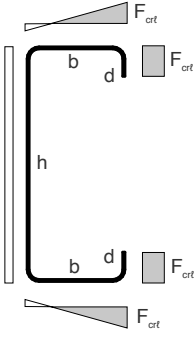
Loading case	Sections without holes			
	SFIA		Non-commercial	
	Mean	COV	Mean	COV
Pure compression	1.00	0.02	1.00	0.02
Major axis bending	0.99	0.05	1.00	0.02
Minor axis bending with lip in compression	1.00	0.06	1.00	0.02
Minor axis bending with lip in tension	1.00	0.02	1.00	0.01

Table 2. Summary of the performance of the proposed equations for sections with standard web punchout

Loading case	With standard web punchout			
	SFIA		Non-commercial	
	Mean	COV	Mean	COV
Pure compression	1.00	0.04	1.00	0.04
Major axis bending	0.99	0.06	1.01	0.05
Minor axis bending with lip in compression	1.01	0.03	1.00	0.02
Minor axis bending with lip in tension	1.00	0.01	1.00	0.02

## 10 Summary of proposed equations

Table 3. List of proposed equations for lipped channels without punchouts

Load case	Geometry	Equation for $F_{crl}$	Proposed k expression
Pure compression		$F_{cr\ell,nh} = k_h \frac{\pi^2 E}{12(1 - v^2)} \left(\frac{t}{h}\right)^2$	$k_h = 4 + \frac{24\eta_h}{20 + 4.4\eta_h + \eta_h^2}$ <p>where  <math>\eta_h = h/b</math>, <math>1.2 \leq \eta_h \leq 22</math></p>
Major axis bending		$F_{cr\ell,nh} = k_b \frac{\pi^2 E}{12(1 - v^2)} \left(\frac{t}{b}\right)^2$ <p>When <math>1 &lt; \eta_h &lt; 2.57</math></p> $F_{cr\ell,nh} = k_h \frac{\pi^2 E}{12(1 - v^2)} \left(\frac{t}{h}\right)^2$ <p>When <math>\eta_h \geq 2.57</math></p>	$k_b = \frac{4.93 - 3.15\eta_h + 0.53\eta_h^2}{1 - 0.64\eta_h + 0.11\eta_h^2}$ $k_h = \frac{-4.3\eta_h + 6.44\eta_h^2}{1 - 0.54\eta_h + 0.24\eta_h^2}$ <p>where  <math>\eta_h = h/b</math>, <math>1.2 \leq \eta_h \leq 22</math></p>
Minor axis bending with lip in compression		$F_{cr\ell,nh} = k_b \frac{\pi^2 E}{12(1 - v^2)} \left(\frac{t}{b}\right)^2$ <p>(Applicable for <math>d/t \geq 4.4</math>)</p>	$k_b = k_{b1} + k_{b2}$ $k_{b1} = 4 + \frac{0.8 - 0.758\eta_b + 0.234\eta_b^2}{1 - 0.533\eta_b + 0.09\eta_b^2}$ $k_{b2} = \begin{cases} 0 & \eta_b \leq 2.75 \\ (4\eta_b - 11)\psi & 2.75 < \eta_b \leq 6 \\ 13\psi & \eta_b > 6 \end{cases}$ <p>where  <math>\eta_b = b/d</math>, <math>2.5 \leq \eta_b \leq 11.1</math>  <math>\psi =  f_2/f_1 </math>, <math>0.07 \leq \psi \leq 0.77</math></p>

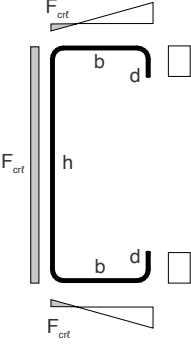
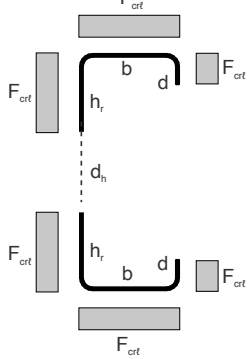
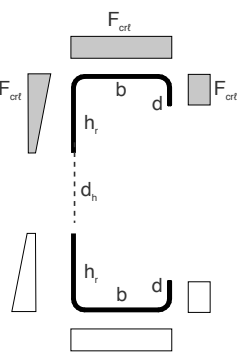
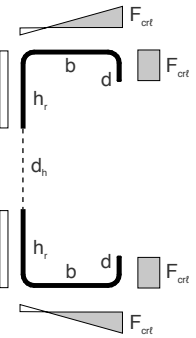
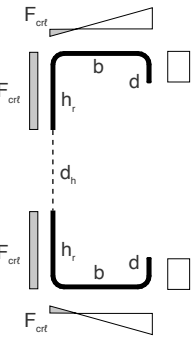
Minor axis bending with lip in tension		$F_{cr\ell,nh} = k_h \frac{\pi^2 E}{12(1 - v^2)} \left(\frac{t}{h}\right)^2$	$k_h = 4 + \frac{1.36 - 0.014\eta_h}{1 - 0.12\eta_h + 0.012\eta_h^2}$ where $\eta_h = h/b, 1.2 \leq \eta_h \leq 22$
--	---	--	---

Table 4. List of proposed equations for lipped channels with standard web punchouts

Load case	Geometry	Equation for $F_{cr\ell,h}$	Proposed k expression
Pure compression		$F_{cr\ell,h} = k_{hr} \frac{\pi^2 E}{12(1 - v^2)} \left(\frac{t}{h_r}\right)^2$	$k_{hr} = C_L k_{hr0}$ $k_{hr0} = \frac{1.02}{1 + 0.04\eta_{hr}^3} \geq 0.43$ $C_L = \frac{0.14 + 0.15p_d}{1 - 0.05p_d} \geq 1$ where $\eta_{hr} = b/h_r, 0.1 \leq \eta_{hr} \leq 3$ $p_d = (d_h/h)^{-1}$
Major axis bending		$F_{cr\ell,h} = k_b \frac{\pi^2 E}{12(1 - v^2)} \left(\frac{t}{b}\right)^2$	$k_b = C_L k_{b0}$ When $\eta_{hrp} < 0.298$ $k_{b0} = \frac{2.952\eta_{hrp}^2}{1 - 2.142\eta_{hrp}}$ When $\eta_{hrp} \geq 0.298$ $k_{b0} = \frac{0.152 + 6.974\eta_{hrp}^3}{1 + 1.277\eta_{hrp}^3}$ $C_L = \frac{0.502 + 0.093p_d^*}{1 - 0.055p_d^*} \geq 1$ where $\eta_{hrp} = (b/h_r)(1 - 0.75\psi),$ $0.1 \leq \eta_{hrp} \leq 2$ $\psi =  f_2/f_1 , 0.09 \leq \psi \leq 0.52$ $p_d^* = (d_h/(h - 0.3b - 0.3d))^{-1}$

---

Minor axis bending with lip in compression		$F_{cr\ell,h} = k_b \frac{\pi^2 E}{12(1 - v^2)} \left(\frac{t}{b}\right)^2$	$k_b = k_{b1} + k_{b2}$ $k_{b1} = 4 + \frac{0.8 - 0.758\eta_b + 0.234\eta_b^2}{1 - 0.533\eta_b + 0.09\eta_b^2}$ $k_{b2} = \begin{cases} 0 & \eta_b \leq 2.75 \\ (4\eta_b - 11)\psi & 2.75 < \eta_b \leq 6 \\ 13\psi & \eta_b > 6 \end{cases}$
Minor axis bending with lip in tension		$F_{cr\ell,h} = k_{hr} \frac{\pi^2 E}{12(1 - v^2)} \left(\frac{t}{h_r}\right)^2$	$k_{hr} = C_L k_{hr0}$ When $\eta_{hr} < 0.4$ $k_{hr0} = \frac{1.15\eta_{hr}}{0.05 + \eta_{hr}} \geq 0.43$ When $\eta_{hr} \geq 0.4$ $k_{hr0} = 1.04 - 0.04\eta_{hr} \geq 0.43$ $C_L = \frac{0.11 + 0.15p_d}{1 - 0.05p_d} \geq 1$

---

## 11 Design examples

### 11.1 Sections without punchouts

#### 11.1.1 Design example 1: 550S162-54 under pure compression

Determine relevant centerline dimensions

$$h = 5.5 - 0.0566 = 5.443 \text{ in.}$$

$$b = 1.625 - 0.0566 = 1.568 \text{ in.}$$

Calculate geometric ratio

$$\eta_h = h/b = 5.443/1.568 = 3.471 (1.2 \leq 3.471 \leq 22 \Rightarrow \text{Good})$$

Calculate buckling coefficient

$$k_{hr} = 4 + \frac{24 \cdot 3.471}{20 + 4.4 \cdot 3.471 + (3.471)^2} = 5.76$$

Calculate critical local buckling stress

$$F_{cr\ell} = 5.76 \frac{\pi^2 29500}{12(1 - 0.3^2)} \left( \frac{0.0566}{5.443} \right)^2 = 16.6 \text{ ksi}$$

In comparison to the FSM result,  $F_{FSM} = 16.7 \text{ ksi}$ , error =  $-0.3\%$

Convert critical buckling stress to load for use in DSM

$$P_{cr\ell} = F_{cr\ell} A = 16.6 \cdot 0.528 = 8.8 \text{ k}$$

### *11.1.2 Design example 2: 800S250-43 under major axis bending*

Determine centerline dimensions

$$h = 8 - 0.0451 = 7.955 \text{ in.}$$

$$b = 2.5 - 0.0451 = 2.455 \text{ in.}$$

Calculate geometric ratio

$$\eta_h = h/b = 7.955/2.455 = 3.240 (1.2 \leq 3.240 \leq 22 \Rightarrow \text{Good})$$

Calculate buckling coefficient

$$k_h = \frac{-4.3 \cdot 3.240 + 6.44 \cdot 3.240^2}{1 - 0.54 \cdot 3.240 + 0.24 \cdot 3.240^2} = 30.33$$

Calculate critical local buckling stress

$$F_{cr\ell} = 30.33 \frac{\pi^2 29500}{12(1 - 0.3^2)} \left( \frac{0.0451}{7.95} \right)^2 = 26.0 \text{ ksi}$$

In comparison to the FSM result,  $F_{FSM} = 25.9 \text{ ksi}$ , error =  $+0.4\%$

Convert critical buckling stress to moment for use in DSM

$$M_{cr\ell} = F_{cr\ell} S_f = 26.0 \cdot 1.512 = 39.3 \text{ in} \cdot \text{k}$$

### *11.1.3 Design example 3: 362S137-33 under minor axis bending with lip in compression*

Determine centerline dimensions

$$b = 1.375 - 0.0346 = 1.340 \text{ in.}$$

$$d = 0.375 - 0.0346/2 = 0.358 \text{ in.}$$

Determine stress gradient

$$\psi = |x_{cg}/(b - x_{cg})| = 0.388/(1.34 - 0.388) = 0.407 (0.07 \leq 0.407 \leq 0.77 \Rightarrow \text{Good})$$

Calculate geometric ratio

$$\eta_b = b/d = 1.340/0.358 = 3.747 (2.5 \leq 3.747 \leq 11.1 \Rightarrow \text{Good})$$

Calculate buckling coefficient

$$k_{b1} = 4 + \frac{0.8 - 0.758 \cdot 3.747 + 0.234 \cdot (3.747)^2}{1 - 0.533 \cdot 3.747 + 0.09 \cdot (3.747)^2} = 8.673$$

$$k_{b2} = (4 \cdot 3.747 - 11) \cdot 0.407 = 1.623$$

$$k_b = k_{b1} + k_{b2} = 8.673 + 1.623 = 10.30$$

Calculate critical local buckling stress

$$F_{cr\ell} = 10.30 \frac{\pi^2 29500}{12(1 - 0.3^2)} \left( \frac{0.0346}{1.340} \right)^2 = 182.9 \text{ ksi}$$

In comparison to the FSM result,  $F_{FSM} = 186.1 \text{ ksi}$ , error =  $-1.7\%$

Convert critical buckling stress to moment for use in DSM

$$M_{cr\ell} = F_{cr\ell} S_f = 186.1 \cdot 0.093 = 46.6 \text{ in} \cdot \text{k}$$

## 11.2 Sections with standard punchouts

### 11.2.1 Design example 4: 550S162-54 with standard web punchout under pure compression

Calculate centerline dimensions

$$h_r = (h - d_h)/2 = (5.443 - 1.5)/2 = 1.972 \text{ in.}$$

Calculate geometric ratios

$$\eta_{hr} = b/h_r = 1.568/1.972 = 0.795 (0.1 \leq 0.795 \leq 3 \Rightarrow \text{Good})$$

$$p_d = (d_h/h)^{-1} = (1.5/5.443)^{-1} = 3.629$$

Determine the unrestrained buckling coefficient  $k_{hr0}$

$$k_{hr0} = \frac{1.02}{1 + 0.04(0.795)^3} = 1.00 > 0.43$$

Determine the multiplier for half wavelength restraint

$$C_L = \frac{0.14 + 0.15(3.629)}{1 - 0.05(3.629)} = 0.836 < 1 \Rightarrow C_L = 1$$

Calculate the full buckling coefficient

$$k_{hr} = C_L k_{hr0} = 1.00 \cdot 1.00 = 1.00$$

Calculate critical local buckling stress

$$F_{cr\ell,h} = 1.00 \frac{\pi^2 29500}{12(1 - 0.3^2)} \left( \frac{0.0566}{1.972} \right)^2 = 22.0 \text{ ksi}$$

In comparison to the FSM result,  $F_{FSM} = 21.8 \text{ ksi}$ , error =  $+0.8\%$

Convert critical local buckling stress to load for use in DSM

$$P_{cr\ell,nh} = 8.8 \text{ k (see Design example 1)}$$

$$P_{cr\ell,h} = F_{cr\ell,h} A_n = 16.6 \cdot 0.443 = 9.7 \text{ k}$$

$$P_{cr\ell} = \min(P_{cr\ell,nh}, P_{cr\ell,h}) = \min(8.8, 9.7) = 8.8 \text{ k (section without hole controls)}$$

### 11.2.2 Design example 5: 800S250-43 with standard web punchout under major axis bending

Calculate centerline dimensions

$$h_r = (h - d_h)/2 = (7.955 - 1.5)/2 = 3.227 \text{ in.}$$

Determine stress gradient

$$\psi = (d_h/2)/(h/2) = (1.5/2)/(7.955/2) = 0.189 (0.09 \leq 0.18 \leq 0.52 \Rightarrow \text{Good})$$

Calculate geometric ratios

$$\eta_{hrp} = (b/h_r)(1 - 0.75\psi) = (2.455/3.227)(1 - 0.75 \cdot 0.189) = 0.653 (0.1 \leq 0.653 \leq 2 \Rightarrow \text{Good})$$

$$p_d^* = (d_h/(h - 0.3b - 0.3d))^{-1} = (1.5/(7.955 - 0.3 \cdot 2.455 - 0.3 \cdot 0.602))^{-1} = 4.692$$

Determine the unrestrained buckling coefficient  $k_{b0}$

Because  $\eta_{hrp} > 0.298$

$$k_{b0} = \frac{0.152 + 6.974(0.653)^3}{1 + 1.277(0.653)^3} = 1.545$$

Determine the multiplier for half-wavelength restraint

$$C_L = \frac{0.502 + 0.093 \cdot 4.692}{1 - 0.055 \cdot 4.692} = 1.265 > 1$$

Calculate the full buckling coefficient

$$k_{hr} = C_L k_{b0} = 1.265 \cdot 1.545 = 1.95$$

Calculate critical local buckling stress

$$F_{cr\ell,h} = 1.95 \frac{\pi^2 29500}{12(1 - 0.3^2)} \left( \frac{0.0451}{7.95} \right)^2 = 17.6 \text{ ksi}$$

In comparison to the FSM result,  $F_{FSM} = 16.2 \text{ ksi}$ , error = +8.2%

Convert critical local buckling stress to moment for use in DSM

$$M_{cr\ell,nh} = 39.3 \text{ in} \cdot \text{k (see Design example 2)}$$

$$M_{cr\ell,h} = F_{cr\ell,h} S_{f,n} = 17.6 \cdot 1.508 = 26.5 \text{ in} \cdot \text{k}$$

$$P_{cr\ell} = \min(M_{cr\ell,nh}, M_{cr\ell,h}) = \min(39.3, 26.5) = 26.5 \text{ k (section with hole controls)}$$

## 12 Conclusions

Analytical equations are proposed for calculating the critical local buckling stress of lipped channel sections with or without web punchouts under compression, major axis bending, and minor axis bending with lips in either compression or tension. Finite strip method analysis is conducted over a wide range of lipped channel sections to generate data for the development of analytical equations. It is found that either or both geometric ratios and stress gradient are the primary factors affecting the local buckling stress of lipped channel sections. Design examples included herein show that the proposed analytical equations are accurate and convenient to use for calculating section local buckling stresses analytically. The proposed equations provide an alternative to the element method in the current AISI specification for calculating local buckling stress, which simplifies the steps required for strength check using the Direct Strength Method (DSM) in the AISI specification.

## Appendix A. Dimensions of non-commercial sections used in FSM analysis

Table 5. Dimensions of the non-commercial sections used in this study

Name	H (in.)	B (in.)	D (in.)	t (in.)	r (in.)
300H50B20D-33	3.00	0.50	0.20	0.0346	0.0765
300H50B20D-43	3.00	0.50	0.20	0.0451	0.0712
300H100B20D-33	3.00	1.00	0.20	0.0346	0.0765
300H100B20D-43	3.00	1.00	0.20	0.0451	0.0712
300H100B40D-33	3.00	1.00	0.40	0.0346	0.0765
300H100B40D-43	3.00	1.00	0.40	0.0451	0.0712
300H100B40D-54	3.00	1.00	0.40	0.0566	0.0849
300H100B40D-68	3.00	1.00	0.40	0.0713	0.107
300H200B20D-33	3.00	2.00	0.20	0.0346	0.0765
300H200B20D-43	3.00	2.00	0.20	0.0451	0.0712
300H200B40D-33	3.00	2.00	0.40	0.0346	0.0765
300H200B40D-43	3.00	2.00	0.40	0.0451	0.0712
300H200B40D-54	3.00	2.00	0.40	0.0566	0.0849
300H200B40D-68	3.00	2.00	0.40	0.0713	0.107
300H200B60D-33	3.00	2.00	0.60	0.0346	0.0765
300H200B60D-43	3.00	2.00	0.60	0.0451	0.0712
300H200B60D-54	3.00	2.00	0.60	0.0566	0.0849
300H200B60D-68	3.00	2.00	0.60	0.0713	0.107
300H200B60D-97	3.00	2.00	0.60	0.1017	0.1526
300H200B60D-118	3.00	2.00	0.60	0.1242	0.1863
300H200B80D-33	3.00	2.00	0.80	0.0346	0.0765
300H200B80D-43	3.00	2.00	0.80	0.0451	0.0712
300H200B80D-54	3.00	2.00	0.80	0.0566	0.0849
300H200B80D-68	3.00	2.00	0.80	0.0713	0.107
300H200B80D-97	3.00	2.00	0.80	0.1017	0.1526
300H200B80D-118	3.00	2.00	0.80	0.1242	0.1863
400H50B20D-33	4.00	0.50	0.20	0.0346	0.0765
400H50B20D-43	4.00	0.50	0.20	0.0451	0.0712

400H100B20D-33	4.00	1.00	0.20	0.0346	0.0765
400H100B20D-43	4.00	1.00	0.20	0.0451	0.0712
400H100B40D-33	4.00	1.00	0.40	0.0346	0.0765
400H100B40D-43	4.00	1.00	0.40	0.0451	0.0712
400H100B40D-54	4.00	1.00	0.40	0.0566	0.0849
400H100B40D-68	4.00	1.00	0.40	0.0713	0.107
400H200B20D-33	4.00	2.00	0.20	0.0346	0.0765
400H200B20D-43	4.00	2.00	0.20	0.0451	0.0712
400H200B40D-33	4.00	2.00	0.40	0.0346	0.0765
400H200B40D-43	4.00	2.00	0.40	0.0451	0.0712
400H200B40D-54	4.00	2.00	0.40	0.0566	0.0849
400H200B40D-68	4.00	2.00	0.40	0.0713	0.107
400H200B60D-33	4.00	2.00	0.60	0.0346	0.0765
400H200B60D-43	4.00	2.00	0.60	0.0451	0.0712
400H200B60D-54	4.00	2.00	0.60	0.0566	0.0849
400H200B60D-68	4.00	2.00	0.60	0.0713	0.107
400H200B60D-97	4.00	2.00	0.60	0.1017	0.1526
400H200B60D-118	4.00	2.00	0.60	0.1242	0.1863
400H200B80D-33	4.00	2.00	0.80	0.0346	0.0765
400H200B80D-43	4.00	2.00	0.80	0.0451	0.0712
400H200B80D-54	4.00	2.00	0.80	0.0566	0.0849
400H200B80D-68	4.00	2.00	0.80	0.0713	0.107
400H200B80D-97	4.00	2.00	0.80	0.1017	0.1526
400H200B80D-118	4.00	2.00	0.80	0.1242	0.1863
400H300B40D-33	4.00	3.00	0.40	0.0346	0.0765
400H300B40D-43	4.00	3.00	0.40	0.0451	0.0712
400H300B40D-54	4.00	3.00	0.40	0.0566	0.0849
400H300B40D-68	4.00	3.00	0.40	0.0713	0.107
400H300B60D-33	4.00	3.00	0.60	0.0346	0.0765
400H300B60D-43	4.00	3.00	0.60	0.0451	0.0712
400H300B60D-54	4.00	3.00	0.60	0.0566	0.0849
400H300B60D-68	4.00	3.00	0.60	0.0713	0.107
400H300B60D-97	4.00	3.00	0.60	0.1017	0.1526
400H300B60D-118	4.00	3.00	0.60	0.1242	0.1863
400H300B80D-33	4.00	3.00	0.80	0.0346	0.0765
400H300B80D-43	4.00	3.00	0.80	0.0451	0.0712
400H300B80D-54	4.00	3.00	0.80	0.0566	0.0849
400H300B80D-68	4.00	3.00	0.80	0.0713	0.107
400H300B80D-97	4.00	3.00	0.80	0.1017	0.1526
400H300B80D-118	4.00	3.00	0.80	0.1242	0.1863
400H300B100D-33	4.00	3.00	1.00	0.0346	0.0765
400H300B100D-43	4.00	3.00	1.00	0.0451	0.0712
400H300B100D-54	4.00	3.00	1.00	0.0566	0.0849
400H300B100D-68	4.00	3.00	1.00	0.0713	0.107
400H300B100D-97	4.00	3.00	1.00	0.1017	0.1526
400H300B100D-118	4.00	3.00	1.00	0.1242	0.1863

400H300B120D-33	4.00	3.00	1.20	0.0346	0.0765
400H300B120D-43	4.00	3.00	1.20	0.0451	0.0712
400H300B120D-54	4.00	3.00	1.20	0.0566	0.0849
400H300B120D-68	4.00	3.00	1.20	0.0713	0.107
400H300B120D-97	4.00	3.00	1.20	0.1017	0.1526
400H300B120D-118	4.00	3.00	1.20	0.1242	0.1863
500H50B20D-33	5.00	0.50	0.20	0.0346	0.0765
500H50B20D-43	5.00	0.50	0.20	0.0451	0.0712
500H100B20D-33	5.00	1.00	0.20	0.0346	0.0765
500H100B20D-43	5.00	1.00	0.20	0.0451	0.0712
500H100B40D-33	5.00	1.00	0.40	0.0346	0.0765
500H100B40D-43	5.00	1.00	0.40	0.0451	0.0712
500H100B40D-54	5.00	1.00	0.40	0.0566	0.0849
500H100B40D-68	5.00	1.00	0.40	0.0713	0.107
500H200B20D-33	5.00	2.00	0.20	0.0346	0.0765
500H200B20D-43	5.00	2.00	0.20	0.0451	0.0712
500H200B40D-33	5.00	2.00	0.40	0.0346	0.0765
500H200B40D-43	5.00	2.00	0.40	0.0451	0.0712
500H200B40D-54	5.00	2.00	0.40	0.0566	0.0849
500H200B40D-68	5.00	2.00	0.40	0.0713	0.107
500H200B60D-33	5.00	2.00	0.60	0.0346	0.0765
500H200B60D-43	5.00	2.00	0.60	0.0451	0.0712
500H200B60D-54	5.00	2.00	0.60	0.0566	0.0849
500H200B60D-68	5.00	2.00	0.60	0.0713	0.107
500H200B60D-97	5.00	2.00	0.60	0.1017	0.1526
500H200B60D-118	5.00	2.00	0.60	0.1242	0.1863
500H200B80D-33	5.00	2.00	0.80	0.0346	0.0765
500H200B80D-43	5.00	2.00	0.80	0.0451	0.0712
500H200B80D-54	5.00	2.00	0.80	0.0566	0.0849
500H200B80D-68	5.00	2.00	0.80	0.0713	0.107
500H200B80D-97	5.00	2.00	0.80	0.1017	0.1526
500H200B80D-118	5.00	2.00	0.80	0.1242	0.1863
500H300B40D-33	5.00	3.00	0.40	0.0346	0.0765
500H300B40D-43	5.00	3.00	0.40	0.0451	0.0712
500H300B40D-54	5.00	3.00	0.40	0.0566	0.0849
500H300B40D-68	5.00	3.00	0.40	0.0713	0.107
500H300B60D-33	5.00	3.00	0.60	0.0346	0.0765
500H300B60D-43	5.00	3.00	0.60	0.0451	0.0712
500H300B60D-54	5.00	3.00	0.60	0.0566	0.0849
500H300B60D-68	5.00	3.00	0.60	0.0713	0.107
500H300B60D-97	5.00	3.00	0.60	0.1017	0.1526
500H300B60D-118	5.00	3.00	0.60	0.1242	0.1863
500H300B80D-33	5.00	3.00	0.80	0.0346	0.0765
500H300B80D-43	5.00	3.00	0.80	0.0451	0.0712
500H300B80D-54	5.00	3.00	0.80	0.0566	0.0849
500H300B80D-68	5.00	3.00	0.80	0.0713	0.107

500H300B80D-97	5.00	3.00	0.80	0.1017	0.1526
500H300B80D-118	5.00	3.00	0.80	0.1242	0.1863
500H300B100D-33	5.00	3.00	1.00	0.0346	0.0765
500H300B100D-43	5.00	3.00	1.00	0.0451	0.0712
500H300B100D-54	5.00	3.00	1.00	0.0566	0.0849
500H300B100D-68	5.00	3.00	1.00	0.0713	0.107
500H300B100D-97	5.00	3.00	1.00	0.1017	0.1526
500H300B100D-118	5.00	3.00	1.00	0.1242	0.1863
500H300B120D-33	5.00	3.00	1.20	0.0346	0.0765
500H300B120D-43	5.00	3.00	1.20	0.0451	0.0712
500H300B120D-54	5.00	3.00	1.20	0.0566	0.0849
500H300B120D-68	5.00	3.00	1.20	0.0713	0.107
500H300B120D-97	5.00	3.00	1.20	0.1017	0.1526
500H300B120D-118	5.00	3.00	1.20	0.1242	0.1863
600H50B20D-33	6.00	0.50	0.20	0.0346	0.0765
600H50B20D-43	6.00	0.50	0.20	0.0451	0.0712
600H100B20D-33	6.00	1.00	0.20	0.0346	0.0765
600H100B20D-43	6.00	1.00	0.20	0.0451	0.0712
600H100B40D-33	6.00	1.00	0.40	0.0346	0.0765
600H100B40D-43	6.00	1.00	0.40	0.0451	0.0712
600H100B40D-54	6.00	1.00	0.40	0.0566	0.0849
600H100B40D-68	6.00	1.00	0.40	0.0713	0.107
600H200B20D-33	6.00	2.00	0.20	0.0346	0.0765
600H200B20D-43	6.00	2.00	0.20	0.0451	0.0712
600H200B40D-33	6.00	2.00	0.40	0.0346	0.0765
600H200B40D-43	6.00	2.00	0.40	0.0451	0.0712
600H200B40D-54	6.00	2.00	0.40	0.0566	0.0849
600H200B40D-68	6.00	2.00	0.40	0.0713	0.107
600H200B60D-33	6.00	2.00	0.60	0.0346	0.0765
600H200B60D-43	6.00	2.00	0.60	0.0451	0.0712
600H200B60D-54	6.00	2.00	0.60	0.0566	0.0849
600H200B60D-68	6.00	2.00	0.60	0.0713	0.107
600H200B60D-97	6.00	2.00	0.60	0.1017	0.1526
600H200B60D-118	6.00	2.00	0.60	0.1242	0.1863
600H200B80D-33	6.00	2.00	0.80	0.0346	0.0765
600H200B80D-43	6.00	2.00	0.80	0.0451	0.0712
600H200B80D-54	6.00	2.00	0.80	0.0566	0.0849
600H200B80D-68	6.00	2.00	0.80	0.0713	0.107
600H200B80D-97	6.00	2.00	0.80	0.1017	0.1526
600H200B80D-118	6.00	2.00	0.80	0.1242	0.1863
600H300B40D-33	6.00	3.00	0.40	0.0346	0.0765
600H300B40D-43	6.00	3.00	0.40	0.0451	0.0712
600H300B40D-54	6.00	3.00	0.40	0.0566	0.0849
600H300B40D-68	6.00	3.00	0.40	0.0713	0.107
600H300B60D-33	6.00	3.00	0.60	0.0346	0.0765
600H300B60D-43	6.00	3.00	0.60	0.0451	0.0712

600H300B60D-54	6.00	3.00	0.60	0.0566	0.0849
600H300B60D-68	6.00	3.00	0.60	0.0713	0.107
600H300B60D-97	6.00	3.00	0.60	0.1017	0.1526
600H300B60D-118	6.00	3.00	0.60	0.1242	0.1863
600H300B80D-33	6.00	3.00	0.80	0.0346	0.0765
600H300B80D-43	6.00	3.00	0.80	0.0451	0.0712
600H300B80D-54	6.00	3.00	0.80	0.0566	0.0849
600H300B80D-68	6.00	3.00	0.80	0.0713	0.107
600H300B80D-97	6.00	3.00	0.80	0.1017	0.1526
600H300B80D-118	6.00	3.00	0.80	0.1242	0.1863
600H300B100D-33	6.00	3.00	1.00	0.0346	0.0765
600H300B100D-43	6.00	3.00	1.00	0.0451	0.0712
600H300B100D-54	6.00	3.00	1.00	0.0566	0.0849
600H300B100D-68	6.00	3.00	1.00	0.0713	0.107
600H300B100D-97	6.00	3.00	1.00	0.1017	0.1526
600H300B100D-118	6.00	3.00	1.00	0.1242	0.1863
600H300B120D-33	6.00	3.00	1.20	0.0346	0.0765
600H300B120D-43	6.00	3.00	1.20	0.0451	0.0712
600H300B120D-54	6.00	3.00	1.20	0.0566	0.0849
600H300B120D-68	6.00	3.00	1.20	0.0713	0.107
600H300B120D-97	6.00	3.00	1.20	0.1017	0.1526
600H300B120D-118	6.00	3.00	1.20	0.1242	0.1863
600H400B40D-33	6.00	4.00	0.40	0.0346	0.0765
600H400B40D-43	6.00	4.00	0.40	0.0451	0.0712
600H400B40D-54	6.00	4.00	0.40	0.0566	0.0849
600H400B40D-68	6.00	4.00	0.40	0.0713	0.107
600H400B60D-33	6.00	4.00	0.60	0.0346	0.0765
600H400B60D-43	6.00	4.00	0.60	0.0451	0.0712
600H400B60D-54	6.00	4.00	0.60	0.0566	0.0849
600H400B60D-68	6.00	4.00	0.60	0.0713	0.107
600H400B60D-97	6.00	4.00	0.60	0.1017	0.1526
600H400B60D-118	6.00	4.00	0.60	0.1242	0.1863
600H400B80D-33	6.00	4.00	0.80	0.0346	0.0765
600H400B80D-43	6.00	4.00	0.80	0.0451	0.0712
600H400B80D-54	6.00	4.00	0.80	0.0566	0.0849
600H400B80D-68	6.00	4.00	0.80	0.0713	0.107
600H400B80D-97	6.00	4.00	0.80	0.1017	0.1526
600H400B80D-118	6.00	4.00	0.80	0.1242	0.1863
600H400B100D-33	6.00	4.00	1.00	0.0346	0.0765
600H400B100D-43	6.00	4.00	1.00	0.0451	0.0712
600H400B100D-54	6.00	4.00	1.00	0.0566	0.0849
600H400B100D-68	6.00	4.00	1.00	0.0713	0.107
600H400B100D-97	6.00	4.00	1.00	0.1017	0.1526
600H400B100D-118	6.00	4.00	1.00	0.1242	0.1863
600H400B120D-33	6.00	4.00	1.20	0.0346	0.0765
600H400B120D-43	6.00	4.00	1.20	0.0451	0.0712

600H400B120D-54	6.00	4.00	1.20	0.0566	0.0849
600H400B120D-68	6.00	4.00	1.20	0.0713	0.107
600H400B120D-97	6.00	4.00	1.20	0.1017	0.1526
600H400B120D-118	6.00	4.00	1.20	0.1242	0.1863
600H400B140D-33	6.00	4.00	1.40	0.0346	0.0765
600H400B140D-43	6.00	4.00	1.40	0.0451	0.0712
600H400B140D-54	6.00	4.00	1.40	0.0566	0.0849
600H400B140D-68	6.00	4.00	1.40	0.0713	0.107
600H400B140D-97	6.00	4.00	1.40	0.1017	0.1526
600H400B140D-118	6.00	4.00	1.40	0.1242	0.1863
600H400B160D-33	6.00	4.00	1.60	0.0346	0.0765
600H400B160D-43	6.00	4.00	1.60	0.0451	0.0712
600H400B160D-54	6.00	4.00	1.60	0.0566	0.0849
600H400B160D-68	6.00	4.00	1.60	0.0713	0.107
600H400B160D-97	6.00	4.00	1.60	0.1017	0.1526
600H400B160D-118	6.00	4.00	1.60	0.1242	0.1863
800H50B20D-33	8.00	0.50	0.20	0.0346	0.0765
800H50B20D-43	8.00	0.50	0.20	0.0451	0.0712
800H100B20D-33	8.00	1.00	0.20	0.0346	0.0765
800H100B20D-43	8.00	1.00	0.20	0.0451	0.0712
800H100B40D-33	8.00	1.00	0.40	0.0346	0.0765
800H100B40D-43	8.00	1.00	0.40	0.0451	0.0712
800H100B40D-54	8.00	1.00	0.40	0.0566	0.0849
800H100B40D-68	8.00	1.00	0.40	0.0713	0.107
800H200B20D-33	8.00	2.00	0.20	0.0346	0.0765
800H200B20D-43	8.00	2.00	0.20	0.0451	0.0712
800H200B40D-33	8.00	2.00	0.40	0.0346	0.0765
800H200B40D-43	8.00	2.00	0.40	0.0451	0.0712
800H200B40D-54	8.00	2.00	0.40	0.0566	0.0849
800H200B40D-68	8.00	2.00	0.40	0.0713	0.107
800H200B60D-33	8.00	2.00	0.60	0.0346	0.0765
800H200B60D-43	8.00	2.00	0.60	0.0451	0.0712
800H200B60D-54	8.00	2.00	0.60	0.0566	0.0849
800H200B60D-68	8.00	2.00	0.60	0.0713	0.107
800H200B60D-97	8.00	2.00	0.60	0.1017	0.1526
800H200B60D-118	8.00	2.00	0.60	0.1242	0.1863
800H200B80D-33	8.00	2.00	0.80	0.0346	0.0765
800H200B80D-43	8.00	2.00	0.80	0.0451	0.0712
800H200B80D-54	8.00	2.00	0.80	0.0566	0.0849
800H200B80D-68	8.00	2.00	0.80	0.0713	0.107
800H200B80D-97	8.00	2.00	0.80	0.1017	0.1526
800H200B80D-118	8.00	2.00	0.80	0.1242	0.1863
800H300B40D-33	8.00	3.00	0.40	0.0346	0.0765
800H300B40D-43	8.00	3.00	0.40	0.0451	0.0712
800H300B40D-54	8.00	3.00	0.40	0.0566	0.0849
800H300B40D-68	8.00	3.00	0.40	0.0713	0.107

800H300B60D-33	8.00	3.00	0.60	0.0346	0.0765
800H300B60D-43	8.00	3.00	0.60	0.0451	0.0712
800H300B60D-54	8.00	3.00	0.60	0.0566	0.0849
800H300B60D-68	8.00	3.00	0.60	0.0713	0.107
800H300B60D-97	8.00	3.00	0.60	0.1017	0.1526
800H300B60D-118	8.00	3.00	0.60	0.1242	0.1863
800H300B80D-33	8.00	3.00	0.80	0.0346	0.0765
800H300B80D-43	8.00	3.00	0.80	0.0451	0.0712
800H300B80D-54	8.00	3.00	0.80	0.0566	0.0849
800H300B80D-68	8.00	3.00	0.80	0.0713	0.107
800H300B80D-97	8.00	3.00	0.80	0.1017	0.1526
800H300B80D-118	8.00	3.00	0.80	0.1242	0.1863
800H300B100D-33	8.00	3.00	1.00	0.0346	0.0765
800H300B100D-43	8.00	3.00	1.00	0.0451	0.0712
800H300B100D-54	8.00	3.00	1.00	0.0566	0.0849
800H300B100D-68	8.00	3.00	1.00	0.0713	0.107
800H300B100D-97	8.00	3.00	1.00	0.1017	0.1526
800H300B100D-118	8.00	3.00	1.00	0.1242	0.1863
800H300B120D-33	8.00	3.00	1.20	0.0346	0.0765
800H300B120D-43	8.00	3.00	1.20	0.0451	0.0712
800H300B120D-54	8.00	3.00	1.20	0.0566	0.0849
800H300B120D-68	8.00	3.00	1.20	0.0713	0.107
800H300B120D-97	8.00	3.00	1.20	0.1017	0.1526
800H300B120D-118	8.00	3.00	1.20	0.1242	0.1863
800H400B40D-33	8.00	4.00	0.40	0.0346	0.0765
800H400B40D-43	8.00	4.00	0.40	0.0451	0.0712
800H400B40D-54	8.00	4.00	0.40	0.0566	0.0849
800H400B40D-68	8.00	4.00	0.40	0.0713	0.107
800H400B60D-33	8.00	4.00	0.60	0.0346	0.0765
800H400B60D-43	8.00	4.00	0.60	0.0451	0.0712
800H400B60D-54	8.00	4.00	0.60	0.0566	0.0849
800H400B60D-68	8.00	4.00	0.60	0.0713	0.107
800H400B60D-97	8.00	4.00	0.60	0.1017	0.1526
800H400B60D-118	8.00	4.00	0.60	0.1242	0.1863
800H400B80D-33	8.00	4.00	0.80	0.0346	0.0765
800H400B80D-43	8.00	4.00	0.80	0.0451	0.0712
800H400B80D-54	8.00	4.00	0.80	0.0566	0.0849
800H400B80D-68	8.00	4.00	0.80	0.0713	0.107
800H400B80D-97	8.00	4.00	0.80	0.1017	0.1526
800H400B80D-118	8.00	4.00	0.80	0.1242	0.1863
800H400B100D-33	8.00	4.00	1.00	0.0346	0.0765
800H400B100D-43	8.00	4.00	1.00	0.0451	0.0712
800H400B100D-54	8.00	4.00	1.00	0.0566	0.0849
800H400B100D-68	8.00	4.00	1.00	0.0713	0.107
800H400B100D-97	8.00	4.00	1.00	0.1017	0.1526
800H400B100D-118	8.00	4.00	1.00	0.1242	0.1863

800H400B120D-33	8.00	4.00	1.20	0.0346	0.0765
800H400B120D-43	8.00	4.00	1.20	0.0451	0.0712
800H400B120D-54	8.00	4.00	1.20	0.0566	0.0849
800H400B120D-68	8.00	4.00	1.20	0.0713	0.107
800H400B120D-97	8.00	4.00	1.20	0.1017	0.1526
800H400B120D-118	8.00	4.00	1.20	0.1242	0.1863
800H400B140D-33	8.00	4.00	1.40	0.0346	0.0765
800H400B140D-43	8.00	4.00	1.40	0.0451	0.0712
800H400B140D-54	8.00	4.00	1.40	0.0566	0.0849
800H400B140D-68	8.00	4.00	1.40	0.0713	0.107
800H400B140D-97	8.00	4.00	1.40	0.1017	0.1526
800H400B140D-118	8.00	4.00	1.40	0.1242	0.1863
800H400B160D-33	8.00	4.00	1.60	0.0346	0.0765
800H400B160D-43	8.00	4.00	1.60	0.0451	0.0712
800H400B160D-54	8.00	4.00	1.60	0.0566	0.0849
800H400B160D-68	8.00	4.00	1.60	0.0713	0.107
800H400B160D-97	8.00	4.00	1.60	0.1017	0.1526
800H400B160D-118	8.00	4.00	1.60	0.1242	0.1863
800H500B60D-33	8.00	5.00	0.60	0.0346	0.0765
800H500B60D-43	8.00	5.00	0.60	0.0451	0.0712
800H500B60D-54	8.00	5.00	0.60	0.0566	0.0849
800H500B60D-68	8.00	5.00	0.60	0.0713	0.107
800H500B60D-97	8.00	5.00	0.60	0.1017	0.1526
800H500B60D-118	8.00	5.00	0.60	0.1242	0.1863
800H500B80D-33	8.00	5.00	0.80	0.0346	0.0765
800H500B80D-43	8.00	5.00	0.80	0.0451	0.0712
800H500B80D-54	8.00	5.00	0.80	0.0566	0.0849
800H500B80D-68	8.00	5.00	0.80	0.0713	0.107
800H500B80D-97	8.00	5.00	0.80	0.1017	0.1526
800H500B80D-118	8.00	5.00	0.80	0.1242	0.1863
800H500B100D-33	8.00	5.00	1.00	0.0346	0.0765
800H500B100D-43	8.00	5.00	1.00	0.0451	0.0712
800H500B100D-54	8.00	5.00	1.00	0.0566	0.0849
800H500B100D-68	8.00	5.00	1.00	0.0713	0.107
800H500B100D-97	8.00	5.00	1.00	0.1017	0.1526
800H500B100D-118	8.00	5.00	1.00	0.1242	0.1863
800H500B120D-33	8.00	5.00	1.20	0.0346	0.0765
800H500B120D-43	8.00	5.00	1.20	0.0451	0.0712
800H500B120D-54	8.00	5.00	1.20	0.0566	0.0849
800H500B120D-68	8.00	5.00	1.20	0.0713	0.107
800H500B120D-97	8.00	5.00	1.20	0.1017	0.1526
800H500B120D-118	8.00	5.00	1.20	0.1242	0.1863
800H500B140D-33	8.00	5.00	1.40	0.0346	0.0765
800H500B140D-43	8.00	5.00	1.40	0.0451	0.0712
800H500B140D-54	8.00	5.00	1.40	0.0566	0.0849
800H500B140D-68	8.00	5.00	1.40	0.0713	0.107

800H500B140D-97	8.00	5.00	1.40	0.1017	0.1526
800H500B140D-118	8.00	5.00	1.40	0.1242	0.1863
800H500B160D-33	8.00	5.00	1.60	0.0346	0.0765
800H500B160D-43	8.00	5.00	1.60	0.0451	0.0712
800H500B160D-54	8.00	5.00	1.60	0.0566	0.0849
800H500B160D-68	8.00	5.00	1.60	0.0713	0.107
800H500B160D-97	8.00	5.00	1.60	0.1017	0.1526
800H500B160D-118	8.00	5.00	1.60	0.1242	0.1863
800H500B180D-33	8.00	5.00	1.80	0.0346	0.0765
800H500B180D-43	8.00	5.00	1.80	0.0451	0.0712
800H500B180D-54	8.00	5.00	1.80	0.0566	0.0849
800H500B180D-68	8.00	5.00	1.80	0.0713	0.107
800H500B180D-97	8.00	5.00	1.80	0.1017	0.1526
800H500B180D-118	8.00	5.00	1.80	0.1242	0.1863
800H500B200D-33	8.00	5.00	2.00	0.0346	0.0765
800H500B200D-43	8.00	5.00	2.00	0.0451	0.0712
800H500B200D-54	8.00	5.00	2.00	0.0566	0.0849
800H500B200D-68	8.00	5.00	2.00	0.0713	0.107
800H500B200D-97	8.00	5.00	2.00	0.1017	0.1526
800H500B200D-118	8.00	5.00	2.00	0.1242	0.1863
800H600B60D-33	8.00	6.00	0.60	0.0346	0.0765
800H600B60D-43	8.00	6.00	0.60	0.0451	0.0712
800H600B60D-54	8.00	6.00	0.60	0.0566	0.0849
800H600B60D-68	8.00	6.00	0.60	0.0713	0.107
800H600B60D-97	8.00	6.00	0.60	0.1017	0.1526
800H600B60D-118	8.00	6.00	0.60	0.1242	0.1863
800H600B80D-33	8.00	6.00	0.80	0.0346	0.0765
800H600B80D-43	8.00	6.00	0.80	0.0451	0.0712
800H600B80D-54	8.00	6.00	0.80	0.0566	0.0849
800H600B80D-68	8.00	6.00	0.80	0.0713	0.107
800H600B80D-97	8.00	6.00	0.80	0.1017	0.1526
800H600B80D-118	8.00	6.00	0.80	0.1242	0.1863
800H600B100D-33	8.00	6.00	1.00	0.0346	0.0765
800H600B100D-43	8.00	6.00	1.00	0.0451	0.0712
800H600B100D-54	8.00	6.00	1.00	0.0566	0.0849
800H600B100D-68	8.00	6.00	1.00	0.0713	0.107
800H600B100D-97	8.00	6.00	1.00	0.1017	0.1526
800H600B100D-118	8.00	6.00	1.00	0.1242	0.1863
800H600B120D-33	8.00	6.00	1.20	0.0346	0.0765
800H600B120D-43	8.00	6.00	1.20	0.0451	0.0712
800H600B120D-54	8.00	6.00	1.20	0.0566	0.0849
800H600B120D-68	8.00	6.00	1.20	0.0713	0.107
800H600B120D-97	8.00	6.00	1.20	0.1017	0.1526
800H600B120D-118	8.00	6.00	1.20	0.1242	0.1863
800H600B140D-33	8.00	6.00	1.40	0.0346	0.0765
800H600B140D-43	8.00	6.00	1.40	0.0451	0.0712

800H600B140D-54	8.00	6.00	1.40	0.0566	0.0849
800H600B140D-68	8.00	6.00	1.40	0.0713	0.107
800H600B140D-97	8.00	6.00	1.40	0.1017	0.1526
800H600B140D-118	8.00	6.00	1.40	0.1242	0.1863
800H600B160D-33	8.00	6.00	1.60	0.0346	0.0765
800H600B160D-43	8.00	6.00	1.60	0.0451	0.0712
800H600B160D-54	8.00	6.00	1.60	0.0566	0.0849
800H600B160D-68	8.00	6.00	1.60	0.0713	0.107
800H600B160D-97	8.00	6.00	1.60	0.1017	0.1526
800H600B160D-118	8.00	6.00	1.60	0.1242	0.1863
800H600B180D-33	8.00	6.00	1.80	0.0346	0.0765
800H600B180D-43	8.00	6.00	1.80	0.0451	0.0712
800H600B180D-54	8.00	6.00	1.80	0.0566	0.0849
800H600B180D-68	8.00	6.00	1.80	0.0713	0.107
800H600B180D-97	8.00	6.00	1.80	0.1017	0.1526
800H600B180D-118	8.00	6.00	1.80	0.1242	0.1863
800H600B200D-33	8.00	6.00	2.00	0.0346	0.0765
800H600B200D-43	8.00	6.00	2.00	0.0451	0.0712
800H600B200D-54	8.00	6.00	2.00	0.0566	0.0849
800H600B200D-68	8.00	6.00	2.00	0.0713	0.107
800H600B200D-97	8.00	6.00	2.00	0.1017	0.1526
800H600B200D-118	8.00	6.00	2.00	0.1242	0.1863
1000H50B20D-33	10.00	0.50	0.20	0.0346	0.0765
1000H50B20D-43	10.00	0.50	0.20	0.0451	0.0712
1000H100B20D-33	10.00	1.00	0.20	0.0346	0.0765
1000H100B20D-43	10.00	1.00	0.20	0.0451	0.0712
1000H100B40D-33	10.00	1.00	0.40	0.0346	0.0765
1000H100B40D-43	10.00	1.00	0.40	0.0451	0.0712
1000H100B40D-54	10.00	1.00	0.40	0.0566	0.0849
1000H100B40D-68	10.00	1.00	0.40	0.0713	0.107
1000H200B20D-33	10.00	2.00	0.20	0.0346	0.0765
1000H200B20D-43	10.00	2.00	0.20	0.0451	0.0712
1000H200B40D-33	10.00	2.00	0.40	0.0346	0.0765
1000H200B40D-43	10.00	2.00	0.40	0.0451	0.0712
1000H200B40D-54	10.00	2.00	0.40	0.0566	0.0849
1000H200B40D-68	10.00	2.00	0.40	0.0713	0.107
1000H200B60D-33	10.00	2.00	0.60	0.0346	0.0765
1000H200B60D-43	10.00	2.00	0.60	0.0451	0.0712
1000H200B60D-54	10.00	2.00	0.60	0.0566	0.0849
1000H200B60D-68	10.00	2.00	0.60	0.0713	0.107
1000H200B60D-97	10.00	2.00	0.60	0.1017	0.1526
1000H200B60D-118	10.00	2.00	0.60	0.1242	0.1863
1000H200B80D-33	10.00	2.00	0.80	0.0346	0.0765
1000H200B80D-43	10.00	2.00	0.80	0.0451	0.0712
1000H200B80D-54	10.00	2.00	0.80	0.0566	0.0849
1000H200B80D-68	10.00	2.00	0.80	0.0713	0.107

1000H200B80D-97	10.00	2.00	0.80	0.1017	0.1526
1000H200B80D-118	10.00	2.00	0.80	0.1242	0.1863
1000H300B40D-33	10.00	3.00	0.40	0.0346	0.0765
1000H300B40D-43	10.00	3.00	0.40	0.0451	0.0712
1000H300B40D-54	10.00	3.00	0.40	0.0566	0.0849
1000H300B40D-68	10.00	3.00	0.40	0.0713	0.107
1000H300B60D-33	10.00	3.00	0.60	0.0346	0.0765
1000H300B60D-43	10.00	3.00	0.60	0.0451	0.0712
1000H300B60D-54	10.00	3.00	0.60	0.0566	0.0849
1000H300B60D-68	10.00	3.00	0.60	0.0713	0.107
1000H300B60D-97	10.00	3.00	0.60	0.1017	0.1526
1000H300B60D-118	10.00	3.00	0.60	0.1242	0.1863
1000H300B80D-33	10.00	3.00	0.80	0.0346	0.0765
1000H300B80D-43	10.00	3.00	0.80	0.0451	0.0712
1000H300B80D-54	10.00	3.00	0.80	0.0566	0.0849
1000H300B80D-68	10.00	3.00	0.80	0.0713	0.107
1000H300B80D-97	10.00	3.00	0.80	0.1017	0.1526
1000H300B80D-118	10.00	3.00	0.80	0.1242	0.1863
1000H300B100D-33	10.00	3.00	1.00	0.0346	0.0765
1000H300B100D-43	10.00	3.00	1.00	0.0451	0.0712
1000H300B100D-54	10.00	3.00	1.00	0.0566	0.0849
1000H300B100D-68	10.00	3.00	1.00	0.0713	0.107
1000H300B100D-97	10.00	3.00	1.00	0.1017	0.1526
1000H300B100D-118	10.00	3.00	1.00	0.1242	0.1863
1000H300B120D-33	10.00	3.00	1.20	0.0346	0.0765
1000H300B120D-43	10.00	3.00	1.20	0.0451	0.0712
1000H300B120D-54	10.00	3.00	1.20	0.0566	0.0849
1000H300B120D-68	10.00	3.00	1.20	0.0713	0.107
1000H300B120D-97	10.00	3.00	1.20	0.1017	0.1526
1000H300B120D-118	10.00	3.00	1.20	0.1242	0.1863
1000H400B40D-33	10.00	4.00	0.40	0.0346	0.0765
1000H400B40D-43	10.00	4.00	0.40	0.0451	0.0712
1000H400B40D-54	10.00	4.00	0.40	0.0566	0.0849
1000H400B40D-68	10.00	4.00	0.40	0.0713	0.107
1000H400B60D-33	10.00	4.00	0.60	0.0346	0.0765
1000H400B60D-43	10.00	4.00	0.60	0.0451	0.0712
1000H400B60D-54	10.00	4.00	0.60	0.0566	0.0849
1000H400B60D-68	10.00	4.00	0.60	0.0713	0.107
1000H400B60D-97	10.00	4.00	0.60	0.1017	0.1526
1000H400B60D-118	10.00	4.00	0.60	0.1242	0.1863
1000H400B80D-33	10.00	4.00	0.80	0.0346	0.0765
1000H400B80D-43	10.00	4.00	0.80	0.0451	0.0712
1000H400B80D-54	10.00	4.00	0.80	0.0566	0.0849
1000H400B80D-68	10.00	4.00	0.80	0.0713	0.107
1000H400B80D-97	10.00	4.00	0.80	0.1017	0.1526
1000H400B80D-118	10.00	4.00	0.80	0.1242	0.1863

1000H400B100D-33	10.00	4.00	1.00	0.0346	0.0765
1000H400B100D-43	10.00	4.00	1.00	0.0451	0.0712
1000H400B100D-54	10.00	4.00	1.00	0.0566	0.0849
1000H400B100D-68	10.00	4.00	1.00	0.0713	0.107
1000H400B100D-97	10.00	4.00	1.00	0.1017	0.1526
1000H400B100D-118	10.00	4.00	1.00	0.1242	0.1863
1000H400B120D-33	10.00	4.00	1.20	0.0346	0.0765
1000H400B120D-43	10.00	4.00	1.20	0.0451	0.0712
1000H400B120D-54	10.00	4.00	1.20	0.0566	0.0849
1000H400B120D-68	10.00	4.00	1.20	0.0713	0.107
1000H400B120D-97	10.00	4.00	1.20	0.1017	0.1526
1000H400B120D-118	10.00	4.00	1.20	0.1242	0.1863
1000H400B140D-33	10.00	4.00	1.40	0.0346	0.0765
1000H400B140D-43	10.00	4.00	1.40	0.0451	0.0712
1000H400B140D-54	10.00	4.00	1.40	0.0566	0.0849
1000H400B140D-68	10.00	4.00	1.40	0.0713	0.107
1000H400B140D-97	10.00	4.00	1.40	0.1017	0.1526
1000H400B140D-118	10.00	4.00	1.40	0.1242	0.1863
1000H400B160D-33	10.00	4.00	1.60	0.0346	0.0765
1000H400B160D-43	10.00	4.00	1.60	0.0451	0.0712
1000H400B160D-54	10.00	4.00	1.60	0.0566	0.0849
1000H400B160D-68	10.00	4.00	1.60	0.0713	0.107
1000H400B160D-97	10.00	4.00	1.60	0.1017	0.1526
1000H400B160D-118	10.00	4.00	1.60	0.1242	0.1863
1000H500B60D-33	10.00	5.00	0.60	0.0346	0.0765
1000H500B60D-43	10.00	5.00	0.60	0.0451	0.0712
1000H500B60D-54	10.00	5.00	0.60	0.0566	0.0849
1000H500B60D-68	10.00	5.00	0.60	0.0713	0.107
1000H500B60D-97	10.00	5.00	0.60	0.1017	0.1526
1000H500B60D-118	10.00	5.00	0.60	0.1242	0.1863
1000H500B80D-33	10.00	5.00	0.80	0.0346	0.0765
1000H500B80D-43	10.00	5.00	0.80	0.0451	0.0712
1000H500B80D-54	10.00	5.00	0.80	0.0566	0.0849
1000H500B80D-68	10.00	5.00	0.80	0.0713	0.107
1000H500B80D-97	10.00	5.00	0.80	0.1017	0.1526
1000H500B80D-118	10.00	5.00	0.80	0.1242	0.1863
1000H500B100D-33	10.00	5.00	1.00	0.0346	0.0765
1000H500B100D-43	10.00	5.00	1.00	0.0451	0.0712
1000H500B100D-54	10.00	5.00	1.00	0.0566	0.0849
1000H500B100D-68	10.00	5.00	1.00	0.0713	0.107
1000H500B100D-97	10.00	5.00	1.00	0.1017	0.1526
1000H500B100D-118	10.00	5.00	1.00	0.1242	0.1863
1000H500B120D-33	10.00	5.00	1.20	0.0346	0.0765
1000H500B120D-43	10.00	5.00	1.20	0.0451	0.0712
1000H500B120D-54	10.00	5.00	1.20	0.0566	0.0849
1000H500B120D-68	10.00	5.00	1.20	0.0713	0.107

1000H500B120D-97	10.00	5.00	1.20	0.1017	0.1526
1000H500B120D-118	10.00	5.00	1.20	0.1242	0.1863
1000H500B140D-33	10.00	5.00	1.40	0.0346	0.0765
1000H500B140D-43	10.00	5.00	1.40	0.0451	0.0712
1000H500B140D-54	10.00	5.00	1.40	0.0566	0.0849
1000H500B140D-68	10.00	5.00	1.40	0.0713	0.107
1000H500B140D-97	10.00	5.00	1.40	0.1017	0.1526
1000H500B140D-118	10.00	5.00	1.40	0.1242	0.1863
1000H500B160D-33	10.00	5.00	1.60	0.0346	0.0765
1000H500B160D-43	10.00	5.00	1.60	0.0451	0.0712
1000H500B160D-54	10.00	5.00	1.60	0.0566	0.0849
1000H500B160D-68	10.00	5.00	1.60	0.0713	0.107
1000H500B160D-97	10.00	5.00	1.60	0.1017	0.1526
1000H500B160D-118	10.00	5.00	1.60	0.1242	0.1863
1000H500B180D-33	10.00	5.00	1.80	0.0346	0.0765
1000H500B180D-43	10.00	5.00	1.80	0.0451	0.0712
1000H500B180D-54	10.00	5.00	1.80	0.0566	0.0849
1000H500B180D-68	10.00	5.00	1.80	0.0713	0.107
1000H500B180D-97	10.00	5.00	1.80	0.1017	0.1526
1000H500B180D-118	10.00	5.00	1.80	0.1242	0.1863
1000H500B200D-33	10.00	5.00	2.00	0.0346	0.0765
1000H500B200D-43	10.00	5.00	2.00	0.0451	0.0712
1000H500B200D-54	10.00	5.00	2.00	0.0566	0.0849
1000H500B200D-68	10.00	5.00	2.00	0.0713	0.107
1000H500B200D-97	10.00	5.00	2.00	0.1017	0.1526
1000H500B200D-118	10.00	5.00	2.00	0.1242	0.1863
1000H600B60D-33	10.00	6.00	0.60	0.0346	0.0765
1000H600B60D-43	10.00	6.00	0.60	0.0451	0.0712
1000H600B60D-54	10.00	6.00	0.60	0.0566	0.0849
1000H600B60D-68	10.00	6.00	0.60	0.0713	0.107
1000H600B60D-97	10.00	6.00	0.60	0.1017	0.1526
1000H600B60D-118	10.00	6.00	0.60	0.1242	0.1863
1000H600B80D-33	10.00	6.00	0.80	0.0346	0.0765
1000H600B80D-43	10.00	6.00	0.80	0.0451	0.0712
1000H600B80D-54	10.00	6.00	0.80	0.0566	0.0849
1000H600B80D-68	10.00	6.00	0.80	0.0713	0.107
1000H600B80D-97	10.00	6.00	0.80	0.1017	0.1526
1000H600B80D-118	10.00	6.00	0.80	0.1242	0.1863
1000H600B100D-33	10.00	6.00	1.00	0.0346	0.0765
1000H600B100D-43	10.00	6.00	1.00	0.0451	0.0712
1000H600B100D-54	10.00	6.00	1.00	0.0566	0.0849
1000H600B100D-68	10.00	6.00	1.00	0.0713	0.107
1000H600B100D-97	10.00	6.00	1.00	0.1017	0.1526
1000H600B100D-118	10.00	6.00	1.00	0.1242	0.1863
1000H600B120D-33	10.00	6.00	1.20	0.0346	0.0765
1000H600B120D-43	10.00	6.00	1.20	0.0451	0.0712

1000H600B120D-54	10.00	6.00	1.20	0.0566	0.0849
1000H600B120D-68	10.00	6.00	1.20	0.0713	0.107
1000H600B120D-97	10.00	6.00	1.20	0.1017	0.1526
1000H600B120D-118	10.00	6.00	1.20	0.1242	0.1863
1000H600B140D-33	10.00	6.00	1.40	0.0346	0.0765
1000H600B140D-43	10.00	6.00	1.40	0.0451	0.0712
1000H600B140D-54	10.00	6.00	1.40	0.0566	0.0849
1000H600B140D-68	10.00	6.00	1.40	0.0713	0.107
1000H600B140D-97	10.00	6.00	1.40	0.1017	0.1526
1000H600B140D-118	10.00	6.00	1.40	0.1242	0.1863
1000H600B160D-33	10.00	6.00	1.60	0.0346	0.0765
1000H600B160D-43	10.00	6.00	1.60	0.0451	0.0712
1000H600B160D-54	10.00	6.00	1.60	0.0566	0.0849
1000H600B160D-68	10.00	6.00	1.60	0.0713	0.107
1000H600B160D-97	10.00	6.00	1.60	0.1017	0.1526
1000H600B160D-118	10.00	6.00	1.60	0.1242	0.1863
1000H600B180D-33	10.00	6.00	1.80	0.0346	0.0765
1000H600B180D-43	10.00	6.00	1.80	0.0451	0.0712
1000H600B180D-54	10.00	6.00	1.80	0.0566	0.0849
1000H600B180D-68	10.00	6.00	1.80	0.0713	0.107
1000H600B180D-97	10.00	6.00	1.80	0.1017	0.1526
1000H600B180D-118	10.00	6.00	1.80	0.1242	0.1863
1000H600B200D-33	10.00	6.00	2.00	0.0346	0.0765
1000H600B200D-43	10.00	6.00	2.00	0.0451	0.0712
1000H600B200D-54	10.00	6.00	2.00	0.0566	0.0849
1000H600B200D-68	10.00	6.00	2.00	0.0713	0.107
1000H600B200D-97	10.00	6.00	2.00	0.1017	0.1526
1000H600B200D-118	10.00	6.00	2.00	0.1242	0.1863
1200H100B20D-33	12.00	1.00	0.20	0.0346	0.0765
1200H100B20D-43	12.00	1.00	0.20	0.0451	0.0712
1200H100B40D-33	12.00	1.00	0.40	0.0346	0.0765
1200H100B40D-43	12.00	1.00	0.40	0.0451	0.0712
1200H100B40D-54	12.00	1.00	0.40	0.0566	0.0849
1200H100B40D-68	12.00	1.00	0.40	0.0713	0.107
1200H200B20D-33	12.00	2.00	0.20	0.0346	0.0765
1200H200B20D-43	12.00	2.00	0.20	0.0451	0.0712
1200H200B40D-33	12.00	2.00	0.40	0.0346	0.0765
1200H200B40D-43	12.00	2.00	0.40	0.0451	0.0712
1200H200B40D-54	12.00	2.00	0.40	0.0566	0.0849
1200H200B40D-68	12.00	2.00	0.40	0.0713	0.107
1200H200B60D-33	12.00	2.00	0.60	0.0346	0.0765
1200H200B60D-43	12.00	2.00	0.60	0.0451	0.0712
1200H200B60D-54	12.00	2.00	0.60	0.0566	0.0849
1200H200B60D-68	12.00	2.00	0.60	0.0713	0.107
1200H200B60D-97	12.00	2.00	0.60	0.1017	0.1526
1200H200B60D-118	12.00	2.00	0.60	0.1242	0.1863

1200H200B80D-33	12.00	2.00	0.80	0.0346	0.0765
1200H200B80D-43	12.00	2.00	0.80	0.0451	0.0712
1200H200B80D-54	12.00	2.00	0.80	0.0566	0.0849
1200H200B80D-68	12.00	2.00	0.80	0.0713	0.107
1200H200B80D-97	12.00	2.00	0.80	0.1017	0.1526
1200H200B80D-118	12.00	2.00	0.80	0.1242	0.1863
1200H300B40D-33	12.00	3.00	0.40	0.0346	0.0765
1200H300B40D-43	12.00	3.00	0.40	0.0451	0.0712
1200H300B40D-54	12.00	3.00	0.40	0.0566	0.0849
1200H300B40D-68	12.00	3.00	0.40	0.0713	0.107
1200H300B60D-33	12.00	3.00	0.60	0.0346	0.0765
1200H300B60D-43	12.00	3.00	0.60	0.0451	0.0712
1200H300B60D-54	12.00	3.00	0.60	0.0566	0.0849
1200H300B60D-68	12.00	3.00	0.60	0.0713	0.107
1200H300B60D-97	12.00	3.00	0.60	0.1017	0.1526
1200H300B60D-118	12.00	3.00	0.60	0.1242	0.1863
1200H300B80D-33	12.00	3.00	0.80	0.0346	0.0765
1200H300B80D-43	12.00	3.00	0.80	0.0451	0.0712
1200H300B80D-54	12.00	3.00	0.80	0.0566	0.0849
1200H300B80D-68	12.00	3.00	0.80	0.0713	0.107
1200H300B80D-97	12.00	3.00	0.80	0.1017	0.1526
1200H300B80D-118	12.00	3.00	0.80	0.1242	0.1863
1200H300B100D-33	12.00	3.00	1.00	0.0346	0.0765
1200H300B100D-43	12.00	3.00	1.00	0.0451	0.0712
1200H300B100D-54	12.00	3.00	1.00	0.0566	0.0849
1200H300B100D-68	12.00	3.00	1.00	0.0713	0.107
1200H300B100D-97	12.00	3.00	1.00	0.1017	0.1526
1200H300B100D-118	12.00	3.00	1.00	0.1242	0.1863
1200H300B120D-33	12.00	3.00	1.20	0.0346	0.0765
1200H300B120D-43	12.00	3.00	1.20	0.0451	0.0712
1200H300B120D-54	12.00	3.00	1.20	0.0566	0.0849
1200H300B120D-68	12.00	3.00	1.20	0.0713	0.107
1200H300B120D-97	12.00	3.00	1.20	0.1017	0.1526
1200H300B120D-118	12.00	3.00	1.20	0.1242	0.1863
1200H400B40D-33	12.00	4.00	0.40	0.0346	0.0765
1200H400B40D-43	12.00	4.00	0.40	0.0451	0.0712
1200H400B40D-54	12.00	4.00	0.40	0.0566	0.0849
1200H400B40D-68	12.00	4.00	0.40	0.0713	0.107
1200H400B60D-33	12.00	4.00	0.60	0.0346	0.0765
1200H400B60D-43	12.00	4.00	0.60	0.0451	0.0712
1200H400B60D-54	12.00	4.00	0.60	0.0566	0.0849
1200H400B60D-68	12.00	4.00	0.60	0.0713	0.107
1200H400B60D-97	12.00	4.00	0.60	0.1017	0.1526
1200H400B60D-118	12.00	4.00	0.60	0.1242	0.1863
1200H400B80D-33	12.00	4.00	0.80	0.0346	0.0765
1200H400B80D-43	12.00	4.00	0.80	0.0451	0.0712

1200H400B80D-54	12.00	4.00	0.80	0.0566	0.0849
1200H400B80D-68	12.00	4.00	0.80	0.0713	0.107
1200H400B80D-97	12.00	4.00	0.80	0.1017	0.1526
1200H400B80D-118	12.00	4.00	0.80	0.1242	0.1863
1200H400B100D-33	12.00	4.00	1.00	0.0346	0.0765
1200H400B100D-43	12.00	4.00	1.00	0.0451	0.0712
1200H400B100D-54	12.00	4.00	1.00	0.0566	0.0849
1200H400B100D-68	12.00	4.00	1.00	0.0713	0.107
1200H400B100D-97	12.00	4.00	1.00	0.1017	0.1526
1200H400B100D-118	12.00	4.00	1.00	0.1242	0.1863
1200H400B120D-33	12.00	4.00	1.20	0.0346	0.0765
1200H400B120D-43	12.00	4.00	1.20	0.0451	0.0712
1200H400B120D-54	12.00	4.00	1.20	0.0566	0.0849
1200H400B120D-68	12.00	4.00	1.20	0.0713	0.107
1200H400B120D-97	12.00	4.00	1.20	0.1017	0.1526
1200H400B120D-118	12.00	4.00	1.20	0.1242	0.1863
1200H400B140D-33	12.00	4.00	1.40	0.0346	0.0765
1200H400B140D-43	12.00	4.00	1.40	0.0451	0.0712
1200H400B140D-54	12.00	4.00	1.40	0.0566	0.0849
1200H400B140D-68	12.00	4.00	1.40	0.0713	0.107
1200H400B140D-97	12.00	4.00	1.40	0.1017	0.1526
1200H400B140D-118	12.00	4.00	1.40	0.1242	0.1863
1200H400B160D-33	12.00	4.00	1.60	0.0346	0.0765
1200H400B160D-43	12.00	4.00	1.60	0.0451	0.0712
1200H400B160D-54	12.00	4.00	1.60	0.0566	0.0849
1200H400B160D-68	12.00	4.00	1.60	0.0713	0.107
1200H400B160D-97	12.00	4.00	1.60	0.1017	0.1526
1200H400B160D-118	12.00	4.00	1.60	0.1242	0.1863
1200H500B60D-33	12.00	5.00	0.60	0.0346	0.0765
1200H500B60D-43	12.00	5.00	0.60	0.0451	0.0712
1200H500B60D-54	12.00	5.00	0.60	0.0566	0.0849
1200H500B60D-68	12.00	5.00	0.60	0.0713	0.107
1200H500B60D-97	12.00	5.00	0.60	0.1017	0.1526
1200H500B60D-118	12.00	5.00	0.60	0.1242	0.1863
1200H500B80D-33	12.00	5.00	0.80	0.0346	0.0765
1200H500B80D-43	12.00	5.00	0.80	0.0451	0.0712
1200H500B80D-54	12.00	5.00	0.80	0.0566	0.0849
1200H500B80D-68	12.00	5.00	0.80	0.0713	0.107
1200H500B80D-97	12.00	5.00	0.80	0.1017	0.1526
1200H500B80D-118	12.00	5.00	0.80	0.1242	0.1863
1200H500B100D-33	12.00	5.00	1.00	0.0346	0.0765
1200H500B100D-43	12.00	5.00	1.00	0.0451	0.0712
1200H500B100D-54	12.00	5.00	1.00	0.0566	0.0849
1200H500B100D-68	12.00	5.00	1.00	0.0713	0.107
1200H500B100D-97	12.00	5.00	1.00	0.1017	0.1526
1200H500B100D-118	12.00	5.00	1.00	0.1242	0.1863

1200H500B120D-33	12.00	5.00	1.20	0.0346	0.0765
1200H500B120D-43	12.00	5.00	1.20	0.0451	0.0712
1200H500B120D-54	12.00	5.00	1.20	0.0566	0.0849
1200H500B120D-68	12.00	5.00	1.20	0.0713	0.107
1200H500B120D-97	12.00	5.00	1.20	0.1017	0.1526
1200H500B120D-118	12.00	5.00	1.20	0.1242	0.1863
1200H500B140D-33	12.00	5.00	1.40	0.0346	0.0765
1200H500B140D-43	12.00	5.00	1.40	0.0451	0.0712
1200H500B140D-54	12.00	5.00	1.40	0.0566	0.0849
1200H500B140D-68	12.00	5.00	1.40	0.0713	0.107
1200H500B140D-97	12.00	5.00	1.40	0.1017	0.1526
1200H500B140D-118	12.00	5.00	1.40	0.1242	0.1863
1200H500B160D-33	12.00	5.00	1.60	0.0346	0.0765
1200H500B160D-43	12.00	5.00	1.60	0.0451	0.0712
1200H500B160D-54	12.00	5.00	1.60	0.0566	0.0849
1200H500B160D-68	12.00	5.00	1.60	0.0713	0.107
1200H500B160D-97	12.00	5.00	1.60	0.1017	0.1526
1200H500B160D-118	12.00	5.00	1.60	0.1242	0.1863
1200H500B180D-33	12.00	5.00	1.80	0.0346	0.0765
1200H500B180D-43	12.00	5.00	1.80	0.0451	0.0712
1200H500B180D-54	12.00	5.00	1.80	0.0566	0.0849
1200H500B180D-68	12.00	5.00	1.80	0.0713	0.107
1200H500B180D-97	12.00	5.00	1.80	0.1017	0.1526
1200H500B180D-118	12.00	5.00	1.80	0.1242	0.1863
1200H500B200D-33	12.00	5.00	2.00	0.0346	0.0765
1200H500B200D-43	12.00	5.00	2.00	0.0451	0.0712
1200H500B200D-54	12.00	5.00	2.00	0.0566	0.0849
1200H500B200D-68	12.00	5.00	2.00	0.0713	0.107
1200H500B200D-97	12.00	5.00	2.00	0.1017	0.1526
1200H500B200D-118	12.00	5.00	2.00	0.1242	0.1863
1200H600B60D-33	12.00	6.00	0.60	0.0346	0.0765
1200H600B60D-43	12.00	6.00	0.60	0.0451	0.0712
1200H600B60D-54	12.00	6.00	0.60	0.0566	0.0849
1200H600B60D-68	12.00	6.00	0.60	0.0713	0.107
1200H600B60D-97	12.00	6.00	0.60	0.1017	0.1526
1200H600B60D-118	12.00	6.00	0.60	0.1242	0.1863
1200H600B80D-33	12.00	6.00	0.80	0.0346	0.0765
1200H600B80D-43	12.00	6.00	0.80	0.0451	0.0712
1200H600B80D-54	12.00	6.00	0.80	0.0566	0.0849
1200H600B80D-68	12.00	6.00	0.80	0.0713	0.107
1200H600B80D-97	12.00	6.00	0.80	0.1017	0.1526
1200H600B80D-118	12.00	6.00	0.80	0.1242	0.1863
1200H600B100D-33	12.00	6.00	1.00	0.0346	0.0765
1200H600B100D-43	12.00	6.00	1.00	0.0451	0.0712
1200H600B100D-54	12.00	6.00	1.00	0.0566	0.0849
1200H600B100D-68	12.00	6.00	1.00	0.0713	0.107

1200H600B100D-97	12.00	6.00	1.00	0.1017	0.1526
1200H600B100D-118	12.00	6.00	1.00	0.1242	0.1863
1200H600B120D-33	12.00	6.00	1.20	0.0346	0.0765
1200H600B120D-43	12.00	6.00	1.20	0.0451	0.0712
1200H600B120D-54	12.00	6.00	1.20	0.0566	0.0849
1200H600B120D-68	12.00	6.00	1.20	0.0713	0.107
1200H600B120D-97	12.00	6.00	1.20	0.1017	0.1526
1200H600B120D-118	12.00	6.00	1.20	0.1242	0.1863
1200H600B140D-33	12.00	6.00	1.40	0.0346	0.0765
1200H600B140D-43	12.00	6.00	1.40	0.0451	0.0712
1200H600B140D-54	12.00	6.00	1.40	0.0566	0.0849
1200H600B140D-68	12.00	6.00	1.40	0.0713	0.107
1200H600B140D-97	12.00	6.00	1.40	0.1017	0.1526
1200H600B140D-118	12.00	6.00	1.40	0.1242	0.1863
1200H600B160D-33	12.00	6.00	1.60	0.0346	0.0765
1200H600B160D-43	12.00	6.00	1.60	0.0451	0.0712
1200H600B160D-54	12.00	6.00	1.60	0.0566	0.0849
1200H600B160D-68	12.00	6.00	1.60	0.0713	0.107
1200H600B160D-97	12.00	6.00	1.60	0.1017	0.1526
1200H600B160D-118	12.00	6.00	1.60	0.1242	0.1863
1200H600B180D-33	12.00	6.00	1.80	0.0346	0.0765
1200H600B180D-43	12.00	6.00	1.80	0.0451	0.0712
1200H600B180D-54	12.00	6.00	1.80	0.0566	0.0849
1200H600B180D-68	12.00	6.00	1.80	0.0713	0.107
1200H600B180D-97	12.00	6.00	1.80	0.1017	0.1526
1200H600B180D-118	12.00	6.00	1.80	0.1242	0.1863
1200H600B200D-33	12.00	6.00	2.00	0.0346	0.0765
1200H600B200D-43	12.00	6.00	2.00	0.0451	0.0712
1200H600B200D-54	12.00	6.00	2.00	0.0566	0.0849
1200H600B200D-68	12.00	6.00	2.00	0.0713	0.107
1200H600B200D-97	12.00	6.00	2.00	0.1017	0.1526
1200H600B200D-118	12.00	6.00	2.00	0.1242	0.1863
1400H100B20D-33	14.00	1.00	0.20	0.0346	0.0765
1400H100B20D-43	14.00	1.00	0.20	0.0451	0.0712
1400H100B40D-33	14.00	1.00	0.40	0.0346	0.0765
1400H100B40D-43	14.00	1.00	0.40	0.0451	0.0712
1400H100B40D-54	14.00	1.00	0.40	0.0566	0.0849
1400H100B40D-68	14.00	1.00	0.40	0.0713	0.107
1400H200B20D-33	14.00	2.00	0.20	0.0346	0.0765
1400H200B20D-43	14.00	2.00	0.20	0.0451	0.0712
1400H200B40D-33	14.00	2.00	0.40	0.0346	0.0765
1400H200B40D-43	14.00	2.00	0.40	0.0451	0.0712
1400H200B40D-54	14.00	2.00	0.40	0.0566	0.0849
1400H200B40D-68	14.00	2.00	0.40	0.0713	0.107
1400H200B60D-33	14.00	2.00	0.60	0.0346	0.0765
1400H200B60D-43	14.00	2.00	0.60	0.0451	0.0712

1400H200B60D-54	14.00	2.00	0.60	0.0566	0.0849
1400H200B60D-68	14.00	2.00	0.60	0.0713	0.107
1400H200B60D-97	14.00	2.00	0.60	0.1017	0.1526
1400H200B60D-118	14.00	2.00	0.60	0.1242	0.1863
1400H200B80D-33	14.00	2.00	0.80	0.0346	0.0765
1400H200B80D-43	14.00	2.00	0.80	0.0451	0.0712
1400H200B80D-54	14.00	2.00	0.80	0.0566	0.0849
1400H200B80D-68	14.00	2.00	0.80	0.0713	0.107
1400H200B80D-97	14.00	2.00	0.80	0.1017	0.1526
1400H200B80D-118	14.00	2.00	0.80	0.1242	0.1863
1400H300B40D-33	14.00	3.00	0.40	0.0346	0.0765
1400H300B40D-43	14.00	3.00	0.40	0.0451	0.0712
1400H300B40D-54	14.00	3.00	0.40	0.0566	0.0849
1400H300B40D-68	14.00	3.00	0.40	0.0713	0.107
1400H300B60D-33	14.00	3.00	0.60	0.0346	0.0765
1400H300B60D-43	14.00	3.00	0.60	0.0451	0.0712
1400H300B60D-54	14.00	3.00	0.60	0.0566	0.0849
1400H300B60D-68	14.00	3.00	0.60	0.0713	0.107
1400H300B60D-97	14.00	3.00	0.60	0.1017	0.1526
1400H300B60D-118	14.00	3.00	0.60	0.1242	0.1863
1400H300B80D-33	14.00	3.00	0.80	0.0346	0.0765
1400H300B80D-43	14.00	3.00	0.80	0.0451	0.0712
1400H300B80D-54	14.00	3.00	0.80	0.0566	0.0849
1400H300B80D-68	14.00	3.00	0.80	0.0713	0.107
1400H300B80D-97	14.00	3.00	0.80	0.1017	0.1526
1400H300B80D-118	14.00	3.00	0.80	0.1242	0.1863
1400H300B100D-33	14.00	3.00	1.00	0.0346	0.0765
1400H300B100D-43	14.00	3.00	1.00	0.0451	0.0712
1400H300B100D-54	14.00	3.00	1.00	0.0566	0.0849
1400H300B100D-68	14.00	3.00	1.00	0.0713	0.107
1400H300B100D-97	14.00	3.00	1.00	0.1017	0.1526
1400H300B100D-118	14.00	3.00	1.00	0.1242	0.1863
1400H300B120D-33	14.00	3.00	1.20	0.0346	0.0765
1400H300B120D-43	14.00	3.00	1.20	0.0451	0.0712
1400H300B120D-54	14.00	3.00	1.20	0.0566	0.0849
1400H300B120D-68	14.00	3.00	1.20	0.0713	0.107
1400H300B120D-97	14.00	3.00	1.20	0.1017	0.1526
1400H300B120D-118	14.00	3.00	1.20	0.1242	0.1863
1400H400B40D-33	14.00	4.00	0.40	0.0346	0.0765
1400H400B40D-43	14.00	4.00	0.40	0.0451	0.0712
1400H400B40D-54	14.00	4.00	0.40	0.0566	0.0849
1400H400B40D-68	14.00	4.00	0.40	0.0713	0.107
1400H400B60D-33	14.00	4.00	0.60	0.0346	0.0765
1400H400B60D-43	14.00	4.00	0.60	0.0451	0.0712
1400H400B60D-54	14.00	4.00	0.60	0.0566	0.0849
1400H400B60D-68	14.00	4.00	0.60	0.0713	0.107

1400H400B60D-97	14.00	4.00	0.60	0.1017	0.1526
1400H400B60D-118	14.00	4.00	0.60	0.1242	0.1863
1400H400B80D-33	14.00	4.00	0.80	0.0346	0.0765
1400H400B80D-43	14.00	4.00	0.80	0.0451	0.0712
1400H400B80D-54	14.00	4.00	0.80	0.0566	0.0849
1400H400B80D-68	14.00	4.00	0.80	0.0713	0.107
1400H400B80D-97	14.00	4.00	0.80	0.1017	0.1526
1400H400B80D-118	14.00	4.00	0.80	0.1242	0.1863
1400H400B100D-33	14.00	4.00	1.00	0.0346	0.0765
1400H400B100D-43	14.00	4.00	1.00	0.0451	0.0712
1400H400B100D-54	14.00	4.00	1.00	0.0566	0.0849
1400H400B100D-68	14.00	4.00	1.00	0.0713	0.107
1400H400B100D-97	14.00	4.00	1.00	0.1017	0.1526
1400H400B100D-118	14.00	4.00	1.00	0.1242	0.1863
1400H400B120D-33	14.00	4.00	1.20	0.0346	0.0765
1400H400B120D-43	14.00	4.00	1.20	0.0451	0.0712
1400H400B120D-54	14.00	4.00	1.20	0.0566	0.0849
1400H400B120D-68	14.00	4.00	1.20	0.0713	0.107
1400H400B120D-97	14.00	4.00	1.20	0.1017	0.1526
1400H400B120D-118	14.00	4.00	1.20	0.1242	0.1863
1400H400B140D-33	14.00	4.00	1.40	0.0346	0.0765
1400H400B140D-43	14.00	4.00	1.40	0.0451	0.0712
1400H400B140D-54	14.00	4.00	1.40	0.0566	0.0849
1400H400B140D-68	14.00	4.00	1.40	0.0713	0.107
1400H400B140D-97	14.00	4.00	1.40	0.1017	0.1526
1400H400B140D-118	14.00	4.00	1.40	0.1242	0.1863
1400H400B160D-33	14.00	4.00	1.60	0.0346	0.0765
1400H400B160D-43	14.00	4.00	1.60	0.0451	0.0712
1400H400B160D-54	14.00	4.00	1.60	0.0566	0.0849
1400H400B160D-68	14.00	4.00	1.60	0.0713	0.107
1400H400B160D-97	14.00	4.00	1.60	0.1017	0.1526
1400H400B160D-118	14.00	4.00	1.60	0.1242	0.1863
1400H500B60D-33	14.00	5.00	0.60	0.0346	0.0765
1400H500B60D-43	14.00	5.00	0.60	0.0451	0.0712
1400H500B60D-54	14.00	5.00	0.60	0.0566	0.0849
1400H500B60D-68	14.00	5.00	0.60	0.0713	0.107
1400H500B60D-97	14.00	5.00	0.60	0.1017	0.1526
1400H500B60D-118	14.00	5.00	0.60	0.1242	0.1863
1400H500B80D-33	14.00	5.00	0.80	0.0346	0.0765
1400H500B80D-43	14.00	5.00	0.80	0.0451	0.0712
1400H500B80D-54	14.00	5.00	0.80	0.0566	0.0849
1400H500B80D-68	14.00	5.00	0.80	0.0713	0.107
1400H500B80D-97	14.00	5.00	0.80	0.1017	0.1526
1400H500B80D-118	14.00	5.00	0.80	0.1242	0.1863
1400H500B100D-33	14.00	5.00	1.00	0.0346	0.0765
1400H500B100D-43	14.00	5.00	1.00	0.0451	0.0712

1400H500B100D-54	14.00	5.00	1.00	0.0566	0.0849
1400H500B100D-68	14.00	5.00	1.00	0.0713	0.107
1400H500B100D-97	14.00	5.00	1.00	0.1017	0.1526
1400H500B100D-118	14.00	5.00	1.00	0.1242	0.1863
1400H500B120D-33	14.00	5.00	1.20	0.0346	0.0765
1400H500B120D-43	14.00	5.00	1.20	0.0451	0.0712
1400H500B120D-54	14.00	5.00	1.20	0.0566	0.0849
1400H500B120D-68	14.00	5.00	1.20	0.0713	0.107
1400H500B120D-97	14.00	5.00	1.20	0.1017	0.1526
1400H500B120D-118	14.00	5.00	1.20	0.1242	0.1863
1400H500B140D-33	14.00	5.00	1.40	0.0346	0.0765
1400H500B140D-43	14.00	5.00	1.40	0.0451	0.0712
1400H500B140D-54	14.00	5.00	1.40	0.0566	0.0849
1400H500B140D-68	14.00	5.00	1.40	0.0713	0.107
1400H500B140D-97	14.00	5.00	1.40	0.1017	0.1526
1400H500B140D-118	14.00	5.00	1.40	0.1242	0.1863
1400H500B160D-33	14.00	5.00	1.60	0.0346	0.0765
1400H500B160D-43	14.00	5.00	1.60	0.0451	0.0712
1400H500B160D-54	14.00	5.00	1.60	0.0566	0.0849
1400H500B160D-68	14.00	5.00	1.60	0.0713	0.107
1400H500B160D-97	14.00	5.00	1.60	0.1017	0.1526
1400H500B160D-118	14.00	5.00	1.60	0.1242	0.1863
1400H500B180D-33	14.00	5.00	1.80	0.0346	0.0765
1400H500B180D-43	14.00	5.00	1.80	0.0451	0.0712
1400H500B180D-54	14.00	5.00	1.80	0.0566	0.0849
1400H500B180D-68	14.00	5.00	1.80	0.0713	0.107
1400H500B180D-97	14.00	5.00	1.80	0.1017	0.1526
1400H500B180D-118	14.00	5.00	1.80	0.1242	0.1863
1400H500B200D-33	14.00	5.00	2.00	0.0346	0.0765
1400H500B200D-43	14.00	5.00	2.00	0.0451	0.0712
1400H500B200D-54	14.00	5.00	2.00	0.0566	0.0849
1400H500B200D-68	14.00	5.00	2.00	0.0713	0.107
1400H500B200D-97	14.00	5.00	2.00	0.1017	0.1526
1400H500B200D-118	14.00	5.00	2.00	0.1242	0.1863
1400H600B60D-33	14.00	6.00	0.60	0.0346	0.0765
1400H600B60D-43	14.00	6.00	0.60	0.0451	0.0712
1400H600B60D-54	14.00	6.00	0.60	0.0566	0.0849
1400H600B60D-68	14.00	6.00	0.60	0.0713	0.107
1400H600B60D-97	14.00	6.00	0.60	0.1017	0.1526
1400H600B60D-118	14.00	6.00	0.60	0.1242	0.1863
1400H600B80D-33	14.00	6.00	0.80	0.0346	0.0765
1400H600B80D-43	14.00	6.00	0.80	0.0451	0.0712
1400H600B80D-54	14.00	6.00	0.80	0.0566	0.0849
1400H600B80D-68	14.00	6.00	0.80	0.0713	0.107
1400H600B80D-97	14.00	6.00	0.80	0.1017	0.1526
1400H600B80D-118	14.00	6.00	0.80	0.1242	0.1863

1400H600B100D-33	14.00	6.00	1.00	0.0346	0.0765
1400H600B100D-43	14.00	6.00	1.00	0.0451	0.0712
1400H600B100D-54	14.00	6.00	1.00	0.0566	0.0849
1400H600B100D-68	14.00	6.00	1.00	0.0713	0.107
1400H600B100D-97	14.00	6.00	1.00	0.1017	0.1526
1400H600B100D-118	14.00	6.00	1.00	0.1242	0.1863
1400H600B120D-33	14.00	6.00	1.20	0.0346	0.0765
1400H600B120D-43	14.00	6.00	1.20	0.0451	0.0712
1400H600B120D-54	14.00	6.00	1.20	0.0566	0.0849
1400H600B120D-68	14.00	6.00	1.20	0.0713	0.107
1400H600B120D-97	14.00	6.00	1.20	0.1017	0.1526
1400H600B120D-118	14.00	6.00	1.20	0.1242	0.1863
1400H600B140D-33	14.00	6.00	1.40	0.0346	0.0765
1400H600B140D-43	14.00	6.00	1.40	0.0451	0.0712
1400H600B140D-54	14.00	6.00	1.40	0.0566	0.0849
1400H600B140D-68	14.00	6.00	1.40	0.0713	0.107
1400H600B140D-97	14.00	6.00	1.40	0.1017	0.1526
1400H600B140D-118	14.00	6.00	1.40	0.1242	0.1863
1400H600B160D-33	14.00	6.00	1.60	0.0346	0.0765
1400H600B160D-43	14.00	6.00	1.60	0.0451	0.0712
1400H600B160D-54	14.00	6.00	1.60	0.0566	0.0849
1400H600B160D-68	14.00	6.00	1.60	0.0713	0.107
1400H600B160D-97	14.00	6.00	1.60	0.1017	0.1526
1400H600B160D-118	14.00	6.00	1.60	0.1242	0.1863
1400H600B180D-33	14.00	6.00	1.80	0.0346	0.0765
1400H600B180D-43	14.00	6.00	1.80	0.0451	0.0712
1400H600B180D-54	14.00	6.00	1.80	0.0566	0.0849
1400H600B180D-68	14.00	6.00	1.80	0.0713	0.107
1400H600B180D-97	14.00	6.00	1.80	0.1017	0.1526
1400H600B180D-118	14.00	6.00	1.80	0.1242	0.1863
1400H600B200D-33	14.00	6.00	2.00	0.0346	0.0765
1400H600B200D-43	14.00	6.00	2.00	0.0451	0.0712
1400H600B200D-54	14.00	6.00	2.00	0.0566	0.0849
1400H600B200D-68	14.00	6.00	2.00	0.0713	0.107
1400H600B200D-97	14.00	6.00	2.00	0.1017	0.1526
1400H600B200D-118	14.00	6.00	2.00	0.1242	0.1863

## References

- Ahdab, M. D., A. W. Fischer, C. Ding, B. Glauz, and B. W. Schafer. 2022. “Local Buckling Expressions for Lipped Channels.” *Proc. Annu. Stab. Conf.* Denver, Colorado.
- AISI S100. 2020. *North American Specification for the Design of Cold-Formed Steel Structural Members*. AISI S100-20. Washington, DC: American Iron and Steel Institute.

- Gardner, L., A. Fieber, and L. Macorini. 2019. "Formulae for Calculating Elastic Local Buckling Stresses of Full Structural Cross-sections." *Structures*, 17: 2–20.  
<https://doi.org/10.1016/j.istruc.2019.01.012>.
- Li, Z., and B. W. Schafer. 2010. "Application of the finite strip method in cold-formed steel member design." *J. Constr. Steel Res.*, 66 (8–9): 971–980. <https://doi.org/10.1016/j.jcsr.2010.04.001>.
- de Miranda Batista, E. 2010. "Effective section method: A general direct method for the design of steel cold-formed members under local-global buckling interaction." *Thin-Walled Struct.*, 48 (4): 345–356. <https://doi.org/10.1016/j.tws.2009.11.003>.
- Moen, C. D., and B. W. Schafer. 2009. "Elastic buckling of thin plates with holes in compression or bending." *Thin-Walled Struct.*, 47 (12): 1597–1607. <https://doi.org/10.1016/j.tws.2009.05.001>.
- Schafer, B. W. 2020. "CUFSM 5.04—finite strip buckling analysis of thin-walled members." Baltimore, USA: Johns Hopkins University.
- Seif, M., and B. W. Schafer. 2010. "Local buckling of structural steel shapes." *J. Constr. Steel Res.*, 66 (10): 1232–1247. <https://doi.org/10.1016/j.jcsr.2010.03.015>.
- SFIA. 2018. *Technical guide for cold-formed steel framing products*. Falls Church, VA: Steel Framing Industry Association.



**American Iron and Steel Institute**

25 Massachusetts Avenue, NW  
Suite 800  
Washington, DC 20001

[www.steel.org](http://www.steel.org)

Research Report RP-23-01

